HAWAII DEEP WATER CABLE PROGRAM

PHASE II-D

TASK 4

ABRASION-CORROSION STUDIES

ıess and Economic Development

HAWAII DEEP WATER CABLE PROGRAM

PHASE II-D

TASK 4

ABRASION-CORROSION STUDIES

Prepared by

Bruce E. Liebert, KoMoe Htun and Ahmad Tadjvar
of the
Department of Mechanical Engineering
University of Hawaii

and

Jorn Larsen-Basse
of the
George W. Woodruff School of Mechanical Engineering
Georgia Institute of Technology

for

Parsons Hawaii
Hawaiian Electric Company, Inc.
and the
State of Hawaii
Department of Business and Economic Development

AUGUST 1988

CONTENTS

		PAGE
	FOREWORD	3
I.	EXECUTIVE SUMMARY	4
II.	INTRODUCTION	6
III.	RELEVANT OPERATIONAL PARAMETERS	9
	a. Cable Design	9
	b. Failure Criteria	10
	c. Abrasive Counterface	12
	d. Dimensions of Abrading Span	16
	e. Points of Abrasion	17
	f. Excursions and Loads	19
	g. Number of Cycles and Sliding Distance	21
IV.	CORROSION TESTS	23
	a. Corrosion Coupon Tests	23
	b. Tests with Cable Specimens	30
	c. Samples of Armor Wire	32
	d. Summary of Corrosion Data	35
V.	ABRASION TESTS	37
	a. Abrasion by SiC Abrasive Paper	37
	b. Abrasion by Basalt Rocks	46
	c. Abrasion by Crushed Basalt Slurry	51
VI.	CORROSION-EROSION TESTS	56
	a. Erosion by Polyurethane Sheet	56
	b. Erosion by Rock	57
VII.	DAMAGE SCENARIOS	59
	a. Straight Corrosion of Undamaged Cable	59
	b. Straight Corrosion of Damaged Cable	59
	c. Straight Abrasion	60
	d. Combined Effects	61
VIII.	ACKNOWLEDGMENTS	64
IX.	REFERENCES	65

FOREWORD

This Final Report is the combined report for two separate, but closely coordinated research efforts, one conducted at Georgia Institute of Technology and the other at the University of Hawaii. During the course of data evaluation it became apparent that combination of the results was both desirable and necessary, thus the combined report.

I. EXECUTIVE SUMMARY

An assessment is presented of the possibility that the Hawaii Deep Water Cable may be damaged due to abrasion or abrasion-enhanced corrosion. The sites of potential damage are the several steep scarps in the deep water section of the Alenuihaha Channel. It is anticipated that during deployment the cable may become suspended between ledges and moved back and forth by the daily tidal currents.

It has been shown[3] that the cable will fail by fatigue in less than the 30-year design life if the catenary span exceeds 40 m. We therefore set out to determine if abrasion and corrosion, jointly or separately, could result in failure in 30 years of a 40 m or shorter span.

Previously reported corrosion tests in warm and cold seawater at the Natural Energy Laboratory of Hawaii (NELH) were re-examined, additional tests were conducted, and literature data were evaluated. It was found that the cold drawn AISI 1085 armor wire does not crack in seawater by stress corrosion cracking or hydrogen embrittlement; that freely exposed galvanized coatings corrode at a long-term rate of 15-20 μm/y and bare armor wire at about 75 μm/y in surface seawater, 30 μm/y in cold deep ocean water; that the corrosion rate of the zinc increases drastically when it is protecting bare areas of steel; and that for actual cable specimens the polypropylene serving and the bitumen bedding provide excellent protection which slows the rate of corrosion of the zinc coating to about 30% the rate of freely exposed coupons.

Abrasion tests were conducted on lava samples from shore rocks and from pillow basalt rocks dredged from one of the scarps of interest. Wear was measured as functions of applied pressure and distance of travel. Tests at very high contact stresses were made also to determine the wear of the rock when in contact with the steel. Coefficients of friction fall in the range

0.35-0.45 and this determines the relationship between the maximum excursion due to current drag and the contact load against any abrading rock surface at mid-span. These values vary linearly from zero excursion at 540 kg load to 0.133 m at zero load.

Corrosion-erosion tests against rock showed that corrosion in seawater of the surface freshly formed by abrasion contributes significantly to the loss, at least 0.05 μm per pass.

Combining the various damage mechanisms we find a worst-case damage at a contact load of 300 kg, a corresponding excursion of 0.06 m and a 30-year travel of 5 km. Here, the wear is 5 mm, general corrosion is 2 mm, and corrosion erosion 2-2.5 mm, for a total of about 9.3 mm. The radial distance from the outer wire diameter to the outer lead sheath diameter is 14.6 mm. Given these numbers, and given the fact that there is very low probability that the worst case scenario of span length, rock contact length, and daily excursions will appear in actuality, it appears reasonable to expect that the cable will maintain electrical integrity in spite of the combined damage by abrasion, corrosion, and corrosion-erosion. This assessment does not take into account the possible effects of reduction in mechanical strength due to abrasion-corrosion.

II. INTRODUCTION

Stimulated by the oil embargo exploration for geothermal energy was initiated on the island of Hawaii, or the Big Island, in the Hawaiian chain. It resulted in drilling of a successful well which struck a very hot geothermal fluid. A 3 MW pilot plant has been operated for now well over five years on this reservoir. Additional wells have since been completed and it appears that the resource is very large.

A major obstacle in the way of further development of this important energy resource is the distance to market. About 80% of Hawaii's ~ 1 M inhabitants live in and around Honolulu, on the island of Oahu, some 240 km from the Big Island. Almost all of Oahu's 1000 MW power consumption is supplied by imported oil and this island is therefore the obvious market for the electricity generated at the geothermal fields of the Big Island.

The most feasible way of transporting the electricity at the present time is by means of a submarine power cable. This cable must cross the Alenuihaha Channel between the Big Island and the island of Maui, where depths of up to 2,100 m are encountered. Total length of the cable is expected to be some 280 km. One of the possible routes is shown in Fig. 1 for illustration purposes. These conditions require extension of the current technology of high voltage direct current (HVDC) cables in that they are beyond any previously encountered submarine cable conditions. Present HVDC cable technology has been developed to the extent that the deepest and longest cables deployed and in operation are the Skagerak cables, between Norway and Denmark. These cables are deployed at depths of up to 550 m over a distance of 125 km. Recent cable projects approaching the Skagerak cable depth include a project

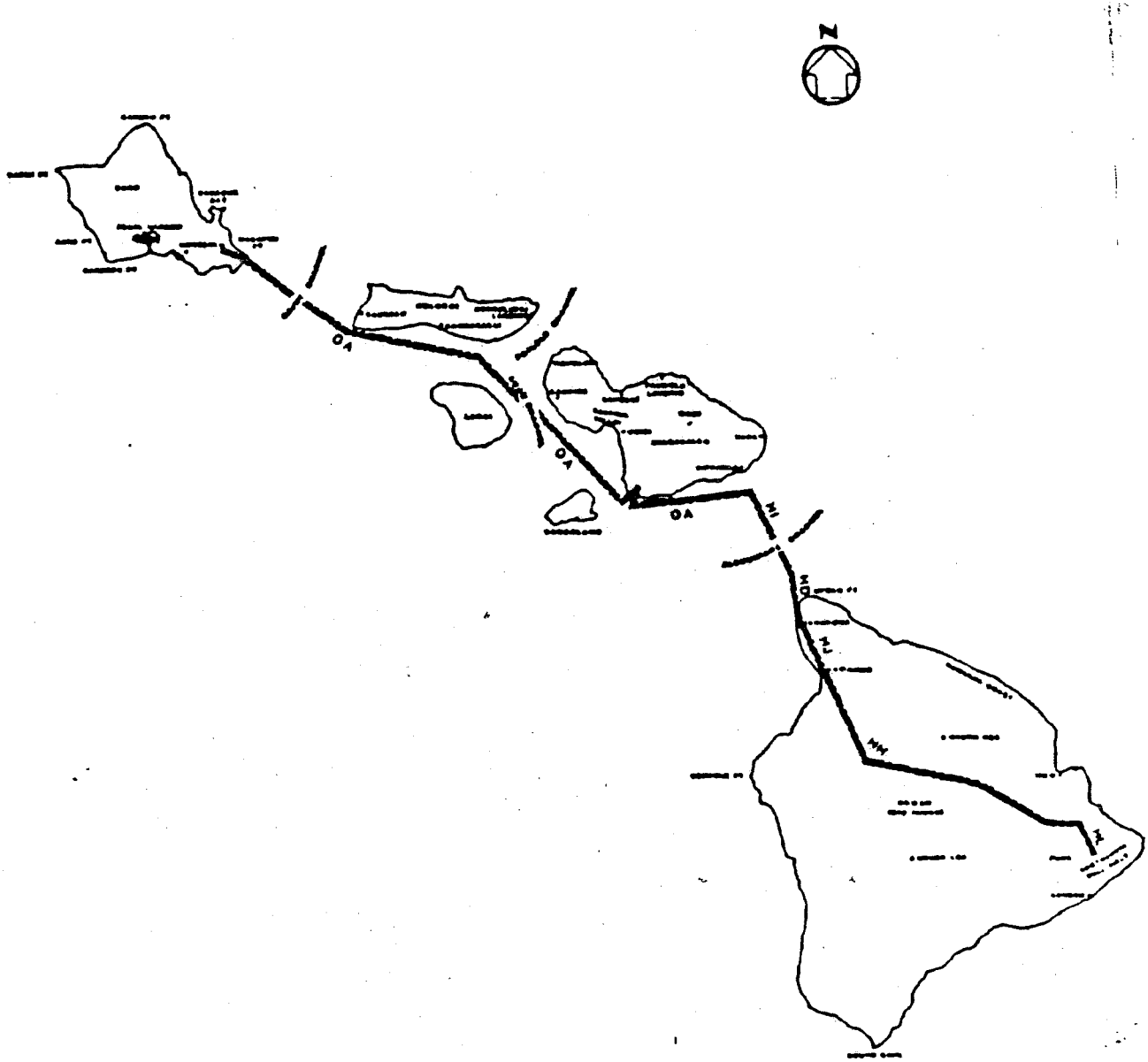

Fig. 1 One of the possible cable routes (1).

in Vancouver, British Columbia and one in the Messina Strait between Italy and Sicily (2). These cables are at depths of 400 and 305 m, respectively.

For the Hawaii cable the subject of abrasive wear takes on importance because it could conceivably be a life-limiting factor. The Alenuihaha Channel is not only the deepest section of the cable route, it is also the most recent, geologically speaking. The bottom is not completely covered with a thick layer of sediment, as is usually the case in the ocean, but exhibits many rock ledges and rock outcroppings from fairly recent submarine volcanic eruptions. Some coral ledges are found also but most ledges are of pillow basalt which contains abrasive mineral grains, such as olivine.

During deployment of the cable, it is expected that sections of it inevitably will become suspended between rock ledges or outcroppings. The substantial tidal currents in the channel will swing the suspended cable section back and forth twice a day, and this may cause abrasive wear against rocks in the vicinity.

It has been estimated (3) that the selected final cable design will fail immediately due to lead sheath fracture, if the span length exceeds 60 m; and that the cable will fail by lead sheath fatigue in less than the desired 30-year life, if the span exceeds 40 m. The question to be answered by these wear tests is if abrasion alone or in combination with corrosion can cause failure sooner than will fatigue.

These concerns were the focus of the present study.

III. RELEVANT OPERATIONAL PARAMETERS

In order to select reasonable test variables it is useful to briefly review the information at hand regarding cable design and environmental as well as operating conditions.

III a. Cable Design

The cable is a so-called self-contained oil filled cable for 300 kV dc current, with aluminum conductors. It is a complex design with a total of 22 different layers. The outermost layers, which are of interest in this connection, are listed in Table 1. The outer diameter is 118.5 mm and the weight is 37 kg/m in air and 27 kg/m in water.

The selected final design is shown in Fig. 2. The materials selection was based on many factors but a major one was the strength to weight ratio, in order to make cable laying feasible at the depths encountered.

TABLE 1
Major Outer Layers in Final Cable Design

	Thickness mm	Outer Dia. mm
Polypropylene yarn serving	3.3	118.4
Outer steel* armor, 31 wires	3.0	111.8
Polypropylene yarn bedding	1.6	105.8
Inner steel* armor, 29 wires	3.0	102.6
Polypropylene yarn bedding	1.1	96.6
Polyethylene jacket	4.0	93.5
Bronze tape	0.6	84.6
Lead sheath	3.3	82.6

*Steel wires are 3 mm x 10 mm, cold drawn galvanized AISI 1085.

III b. Failure Criteria

Abrasion damage can lead to cable failure in two general ways

1) due to water infiltration when the damage penetrates the lead sheath, indicated by line A-A in Fig. 2, or
2) due to mechanical overload (fracture) after significant corrosion and abrasion has taken place, possibly with stresses accentuated while a deep water section of the cable is being retrieved for repair of other damage.

It would appear that condition (1) above is the more commonly expected of the two. It will be used as the tentative failure criterion in this study. For illustration the level of requisite damage is indicated by the line in Fig. 2.

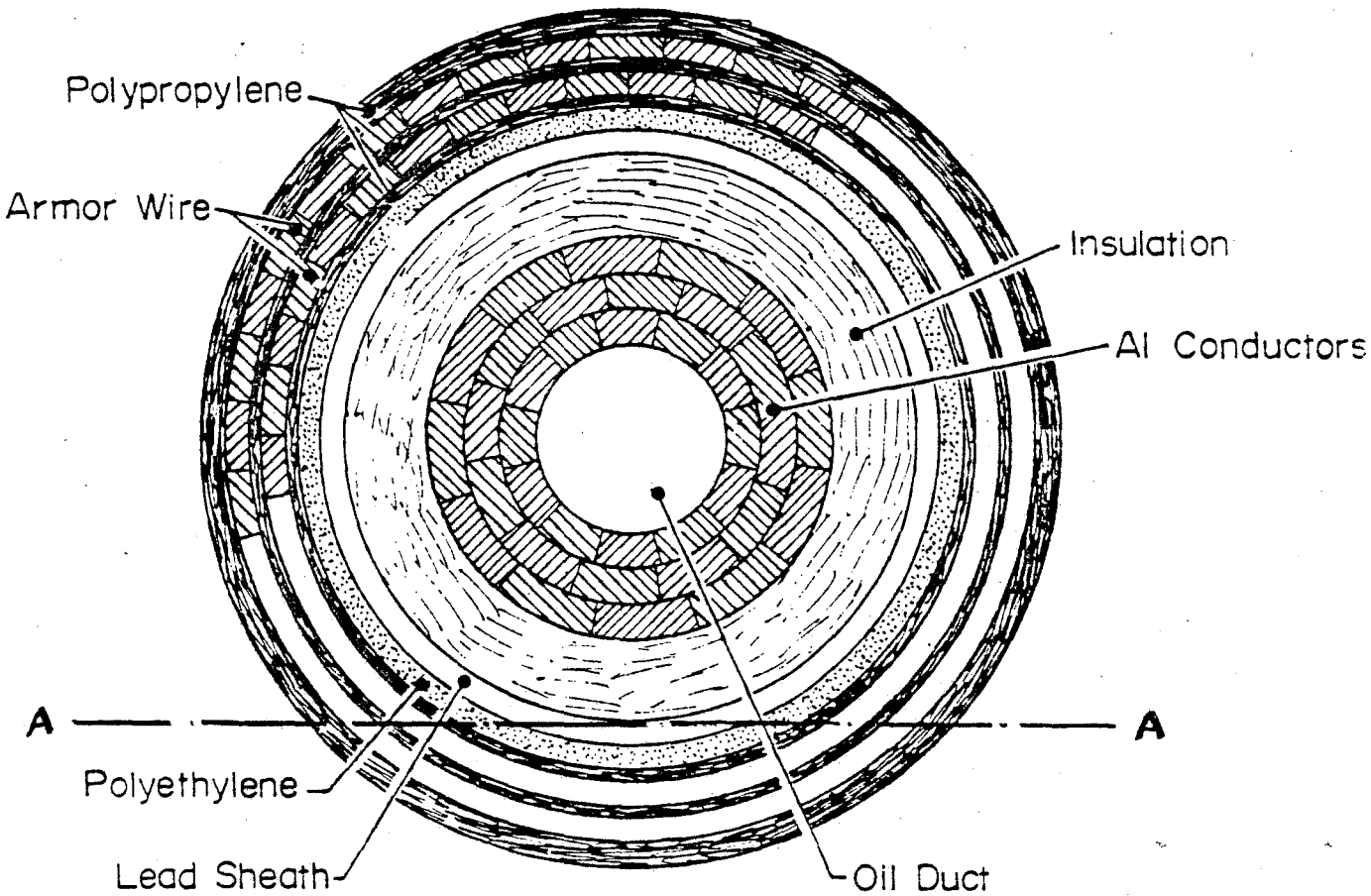

Fig. 2 Cross section of the final cable design. Only the major components are indicated.

III c. Abrasive Counterface

The rocks on the ocean floor will be either coral or pillow basalt from undersea eruptions. The coral is largely soft $CaCO_3$, which is not expected to generate much wear. However, coral rocks usually also contain remains of silica concentrating organisms in small amounts. It is expected that skeleton particles from these organisms will be responsible for most of the abrasion caused by coral.

Lavas and basalts are somewhat more complicated. Their composition, mineralogy, and grain size vary from location to location. The submarine lavas of the cable route are expected to be very similar in composition to the lavas currently being produced by the Kilauea volcano. The most abundant minerals in lava are Pyroxene, Feldspar, and Olivine. A typical lava contains some 48% Pyroxene, 33% Feldspar, 8-10% glassy phase, and 3-6% Olivine (4). Typical hardness values of some of these minerals and some common abrasives are listed in Table 2. Assuming that most wear will be caused by abrasives which are at least 10% harder than the specimen it is seen that all constituents of the lava will abrade the polymers, while only the olivine will abrade a hard steel. In the coral, the silica constituents will probably be responsible for most of the abrasion of both polymers and metals.

TABLE 2

Typical Hardness Values for Some Materials of Interest (4, 5)

Substance	Moh's Scale	Knoop Number	% in Typical Lava	% in Typical Coral
Calcite	3	135	-	98+
Glass		530+	10	-
Pyrotene	5-6	430-560	50	-
Feldspar (orthoclase)	6	560	33	-
Olivine	6,5-7	700-820	6	-
Quartz	7	820	-	1-2
Garnet		1,360		
Alumina	9+	2,100		
Silicon Carbide		2,400		
Steel	5-8	400-750		
Copper	2-3	100-150		
Polymer	1-2	10-100		

The main differences between pillow basalt from deep sea eruptions and lava from surface flows are that the former generally are less porous, due to solidification under pressure, and fine grained due to rapid cooling. They usually have a smooth surface, also due to the rapid cooling.

At-sea surveys of the deeper parts of the Alenuihaha Channel have identified a proposed cable route across this critical section of the total deployment distance (6), see Fig. 3. The survey identified the following bottom conditions, starting from the Kohala side (see Fig. 3).

a-b, shore to coral terrace 6 km offshore at 380 m depth: not investigated,

b-c, large coral terrace, expected to be fairly smooth limestone with occasional pinnacles to 20 m in height,

c-d, 350 m to 850 m, gentle slope of about 2.5 degrees, thin sediment, probably over coral

d-e, 850-950 m, nearly flat with very little sediment

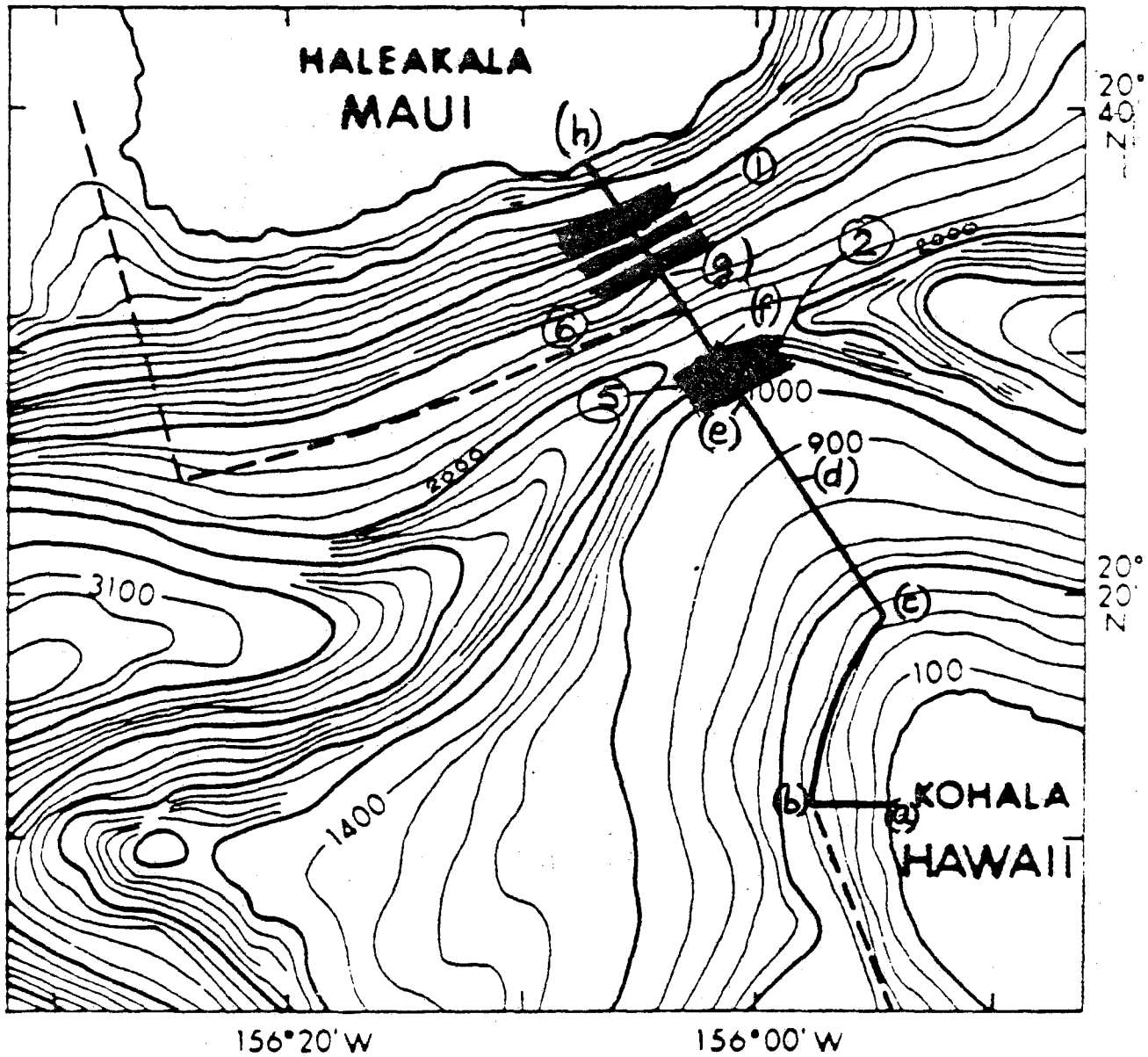

Fig. 3 Suggested route of cable across Alenuihaha channel (6). Numbers refer to dredge samples detailed in (6). Letters refer to discussion in text. Darkened areas are steep scarps where the potential for damage due to abrasion appears greatest.

e-f, 950-1900 m, steep slope of 20 degrees average, but with regions of 35 degrees or greater slope. Lava rock. This was once the shore of the Kohala Volcano. Some coral was found at the upper edge of the slope

f-g, 3-5 km of thick sediment deposits; this section includes the deepest point, which is at about 1925 m,

g-h, the slope up to the Maui coast, average 7 degrees. It consists mostly of gravity flows but has two scarps of volcanic rock at 25 degree slope, or more, at approximately 1500-1300 m and 900-650 m depth. A third such scarp may exist at about 1200 m.

It is expected that if sections of the cable do become suspended as catenaries between rock outcroppings it will most likely happen in the deeper and steeper sections of the route, i.e., at any of the three or four steep lava rock scarps. It has previously been shown (7) that coral generally is much less abrasive than lava; therefore, this study concentrated on abrasion by the types of lava most likely to be found in the scarps.

During the at-sea survey rock dredges were collected at four different points of interest here. These points are shown as numbers 1,2,5 and 6 in Fig. 3. The description of these rocks from (6) is summarized below.

On the Haleakala side

RD 1, 640-850 m depth.
Very massive, dark gray, fine to medium grained lava, probably basalt or hawaiite. Some pieces are coarsely vesicular and almost certainly formed subaerially.

RD 6, 1120-1140 m depth.
Basaltic pillow with thick glassy rind. Piece is aphyric and aphonitic with possible microphenocrysts ($\leq$ 1 mm) of plagioclase. Probably submarine. Samples from this dredge were used in tests described below.

On the Kohala side

RD 2, 1400-1670 m depth.
Three principal rock types - fine grained basaltic pillow, vesicular basalt, and breccia of these two rocks. The pillow fragments are olivine basalt with about 5% fresh euhedral phenocrysts up to 5 mm in size in an aphanitic ground mass. A thin (~ 1 mm) Mn coating is on the surface, which has 2-3 mm glassy rinds. The vesicular basalt has vesicules up to 5 mm in size and is richer in olivine, with

grains up to 5 mm comprising up to 20% of the modal volume. These rocks were probably erupted in shallower water.

RD 5, 1155-1615 m depth
Mostly very olivine-rich basalt (oceanite) with 15-20% olivine phenocrysts up to 15 mm long. Probably formed subaerially. Also some pieces of hyaloclastite with glassy clasts up to 2 cm in diameter. Some of the glassy clasts have olivine phenocrysts up to 4 mm.

In general, then, the rocks of interest are fine grained with occasional large grains of olivine. They have been formed under submarine or subaerial conditions, and thus will have relatively little porosity.

More porous rock with a coarse matrix of the non-olivine mineral components would be expected from surface eruptions. Such rocks may be more abrasive because of the coarser grains and the mechanical locking due to the pores. They may exist in the near-coastal section (a)-(b) and at the top edge of the scarp (e)-(f). In section (a)-(b), which was not investigated, the bottom slope is quite flat and the water depth is relatively low. Therefore, abrasive conditions are not likely to be severe and inspection of the cable laying should be easy. For section (e)-(f) the two dredge samples did not contain any rock from surface eruptions. However, considering that this scarp is the old coastline of the Kohala Volcano, such surface or near-surface rocks may exist over some parts of the scarp.

III d. Dimensions of Abrading Span

The amount of wear due to abrasion depends on the contact load and the distance of sliding. These factors will be estimated below.

In the catenary study (3) mentioned previously, it was estimated that the cable will fail due to overload in bending (radius of curvature greater than 1.5 m) if the span length is greater than 60 m or if the cable hangs over one

outcrop which is more than 4 m high (Fig. 4a). And it will fail in fatigue due to tidal forces in 30 years or less if the span length exceeds 40 m (Fig. 4b). We have used these conditions as the upper limits for the case of failure due to abrasion.

For the calculations the same values as in (3) were used for bottom tension (3000 kg) and flexural modulus (500 kg • m^2, measured for the Vancouver and Messina cables). The vertical force on a span is 27 kg/m (the cable's weight in water) and the horizontal force is due to drag from the tidal currents. Using again the values from (3) this force varies from zero to an average maximum of 7 kg/m. Force balance between these two forces means that the cable can swing an angle of $\tan^{-1}(7/27) = 14.5^{o}$. For the condition shown in Fig. 4b the maximum excursion is at the midpoint and it amounts to 0.47m.

III e. Points of Abrasion

The cable span may conceivably abrade at two types of contact with the rock:

a) at the ends of the span, or

b) at points in between where the contact load is insufficient to provide a span terminus and the contact is of a "grazing" nature.

At the support points for the span in Fig. 4b the vertical force is 20 x 27 kg = 540 kg. The average max. horizontal force is 20 x 7 = 140 kg. Thus, for a coefficient of friction between cable and rock of less than 140/540 = 0.26, the cable will slide at the supports. This value is quite low for abrasive situations, where values of 0.6 - 0.8 are common. Thus, unless

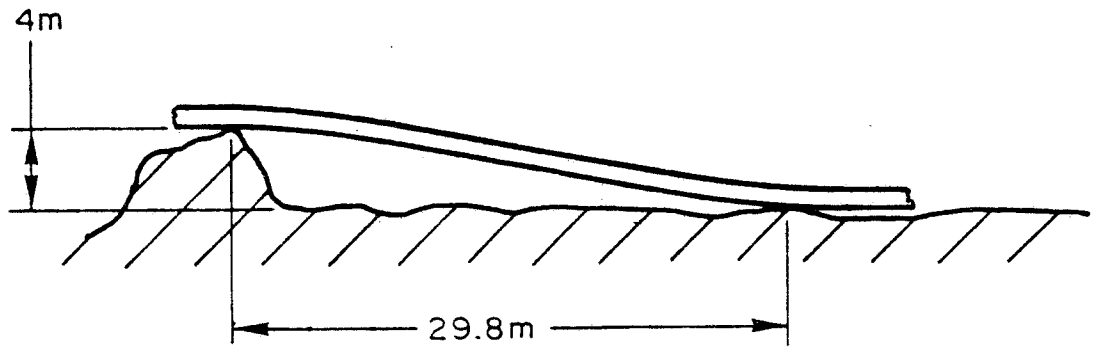

a.

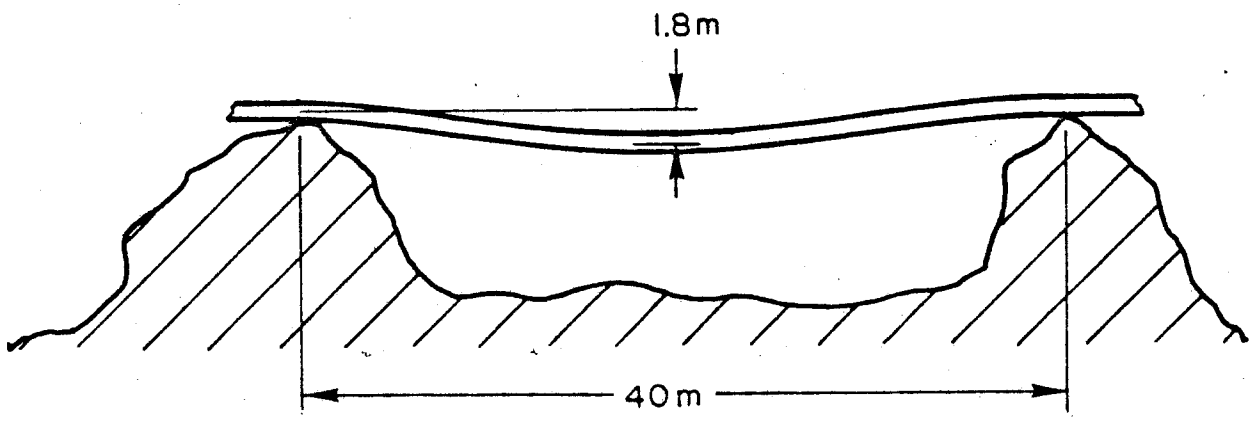

b.

Fig. 4 Sketch of upper-limit conditions for which abrasion becomes a potential failure mechanism. a) The cable will fail due to tension fracture of the sheath if it is deployed over an outcrop which is > 4m above surroundings[3]. The corresponding minimum span length is 29.8 m. b) The cable will fail in 30 years or less by fatigue of the sheath due to tidal current forces if the free span length is > 40 m[3].

actual data show such low friction values, one should not expect the cable to undergo major sliding at the support points.

Some minor sliding could be expected at these points, however. This could occur if there is contact for some distance from the major support point, see Fig. 5b. In the horizontal plane the radius of curvature at the support joint is about 4.45 m for a drag of 7 kg/m. If the contact zone is, say, 0.5 m long, the excursion at the end of that zone is then 2.8 cm.

III f. Excursions and Loads

If abrasion takes place at a mid point of a span, then the excursion at that point depends on the contact load and the coefficient of friction, see Fig. 5a. The friction force at midpoint will counteract movement of the cable in the horizontal plane due to tidal drag. To obtain a rough estimate of the excursion as a function of the friction force the latter has been distributed on the middle 30 m of the 40 m catenary. The drag then is (7 - F/30) kg/m, where F is the friction force. The excursion at mid point then becomes

$$h \simeq \frac{wL^2}{8T_0} = \frac{(7 - F/30) \cdot 40^2}{8 \cdot 3000} \tag{1}$$

$$h = 0.47 - F \cdot 0.0022 \tag{2}$$

where h is in m and F in kg force, and

$$F = \mu N \tag{3}$$

where μ is the coefficient of friction and N is the normal load ($N \leq 540$ kg).

It is realized that this approach is only a rough estimate. It should be sufficient to evaluate the possible abrasive conditions in a worst-case scenario. The calculated excursion-load relations for selected values of μ

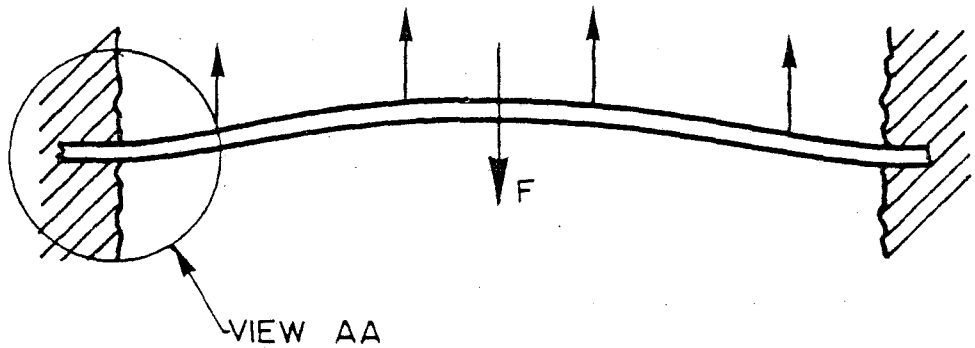

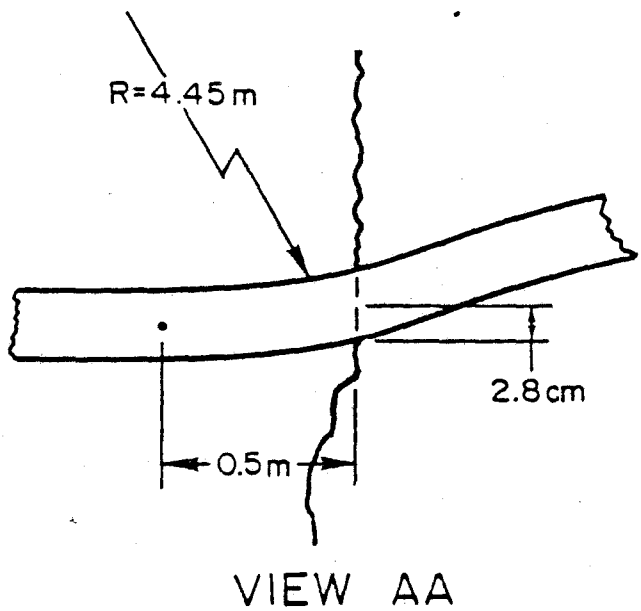

Fig. 5 Top view of catenary exposed to tidal current drag; excursion at mid-point, balance between tidal current drag and possible friction against rock; possible excursion at support point.

are shown in Fig. 6. Quite similar results, but slightly lower, are expected for the case shown in Fig. 4a, where the free span equivalent is about 30 m in length.

III g. Number of Cycles and Sliding Distance

The tidal currents give two complete load cycles per day, or a sliding distance of about 8 times the excursion values calculated above. While the magnitude of the currents varies and there is no significant bottom current for about 10% of the time (3), we have used the full value in these worst-case calculations. In 30 years the max. sliding distance becomes 87,600 x h.

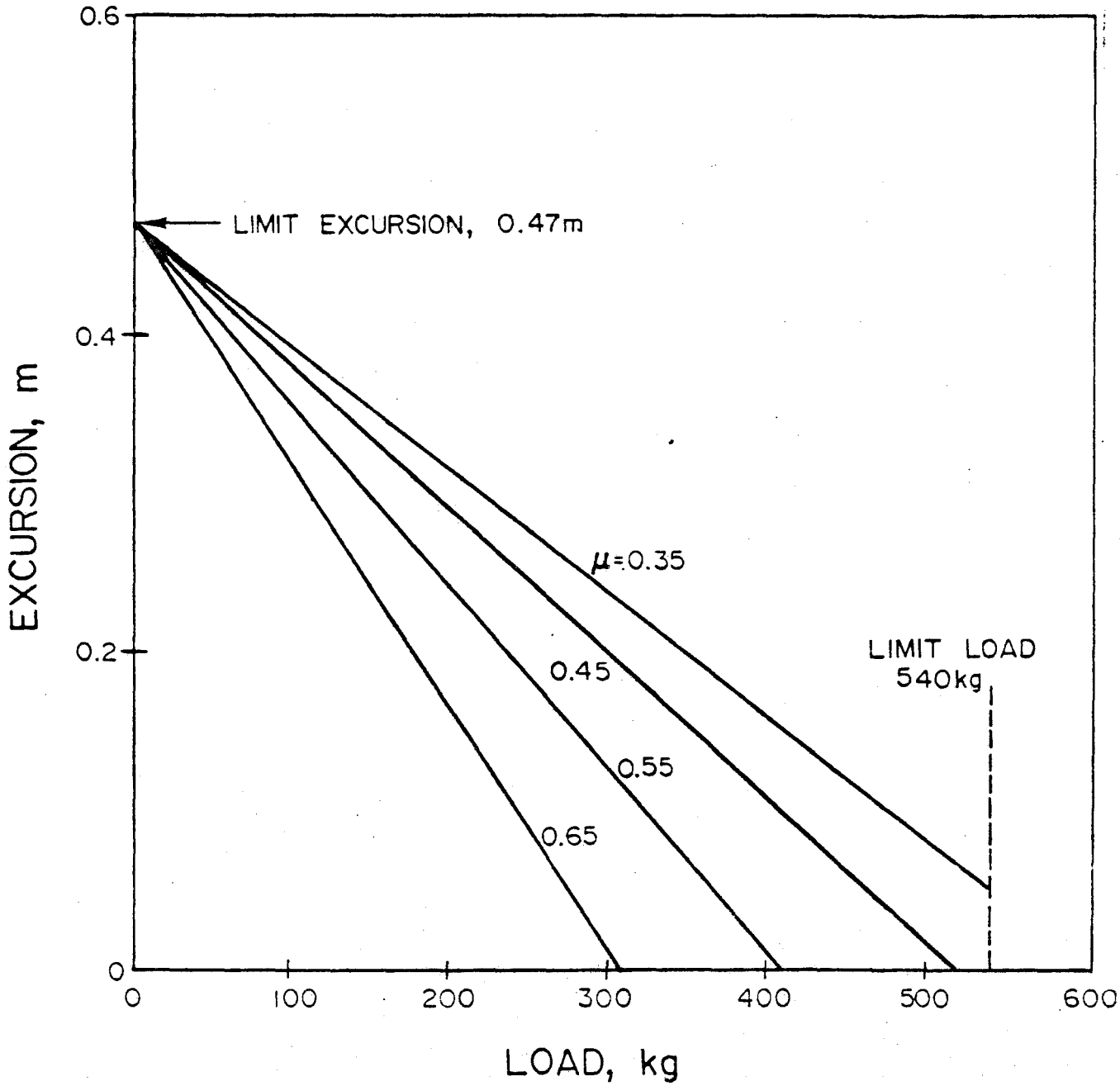

Fig. 6 Estimated mid-point excursions for various levels of contact load and friction coefficient.

IV. CORROSION TESTS

The armor wires will be subjected to corrosion by the surrounding seawater. Steels generally are especially susceptible to attack by sulfate reducing bacteria, which are quite abundant in Hawaiian waters and ocean bottom sediments.

In general, the cold deep ocean seawater is low in oxygen, pH and temperature. It is therefore generally less aggressive towards steels but may be more aggressive towards pH-sensitive metals, such as zinc and aluminum. Tests conducted at the Natural Energy Laboratory of Hawaii (NELH) have permitted a rather extensive evaluation of these effects, at least as they are manifested in relatively short-term exposures. They will be discussed below.

Cable operating temperature is expected to be around 60°C. In the current program phase it has not been possible to determine the corrosivity of deep ocean water, when heated to this temperature. Only some tentative generalizations can be made, based on tests in deep ocean water in the as-is condition, i.e, as it arrives on shore at the NELH.

IV a. Corrosion Coupon Tests

In our report for Phase II B of this project, we presented corrosion data for a number of alloys tested at NELH. Briefly, coupons were exposed in covered troughs on shore at NELH in slowly flowing water. Parallel tests were conducted in warm surface seawater and in cold, deep ocean water pumped from 600 m depth. Exposure times of up to 10 months were used.

These data have been further evaluated, combined with other results from NELH, and compared with literature results (8). The basic findings can be summarized as follows.

- The cold water corrosion rates compare quite closely with data for tests conducted in situ on the bottom at various depths in the Pacific Ocean off Port Hueneme in California.
- There is no significant difference in corrosion rate with depth between 600 and 2100 m.
- Corrosion rates for all samples decrease rapidly with time during the early stage of exposure.
- After 1-3 years most data from around the world for corrosion rates tend towards similar values for individual alloys, and
- The cold deep ocean water is more aggressive than the warm surface water towards zinc, copper, lead and galvanized steel and less aggressive towards steels. This behavior may be due to the low pH of the deep ocean water, which results in rapid attack of pH-sensitive alloys; and to the abundant presence of sulfate reducing bacteria in the surface seawater, which accelerate the corrosion of steels.

For alloys of specific interest in connection with the current effort, the results may be summarized as follows.

Galvanized Steel: The data followed quite closely the expression

$$x = 1.5 \cdot t^{1/2} \tag{4}$$

in the warm water and

$$x = 3.0\ t^{2/3} \tag{5}$$

in the cold. Here, x is the thickness loss, in μm, and t is the exposure time, in days. While the initial corrosion rate in the warm water was greater than in the cold, the latter soon overtook the former. After 10 months 85% of the 45 μm thick coating had disappeared in the cold water and 50-60% had disappeared in the warm water. At this point the remaining zinc still essentially protected the underlying steel.

Comparison with literature data is shown in Fig. 7. The limited deep ocean data indicate that a long term rate of around 20 μm/y (micrometers per year) is established after two years. The surface water data from Hawaii showed lower rates in the beginning than did other waters around the world, possibly because of the high pH. After about two years, however, a universal rate of about 15-20 μm seems to become established.

High-Carbon Steel: Annealed steel AISI 1090 was tested. It followed a similar log-log relation as the galvanized coating, with

$$x = 3.4\ t^{2/3} \tag{6}$$

in the warm water, and

$$x = 5.1\ t^{1/3} \tag{7}$$

in the cold. Comparison with literature data is shown in Fig. 8. This graph also includes data for low alloy steels AISI 4130 and 4340 from the troughs at NELH, as well as data for AISI 1010 tested offshore at NELH in a round-robin ASTM test series. The cold water data coincide with the Port Hueneme deep ocean test results and show that a long-range corrosion rate of 20-40 μm/y becomes established after about one year.

For the warm water the data do not allow confident estimation of long-term rates. It would appear that a rate of around 130 μm/y is established after 3 years. Comparison with results for low carbon steels suggests that the rate may drop to about 50-75 μm/y after 4-5 years.

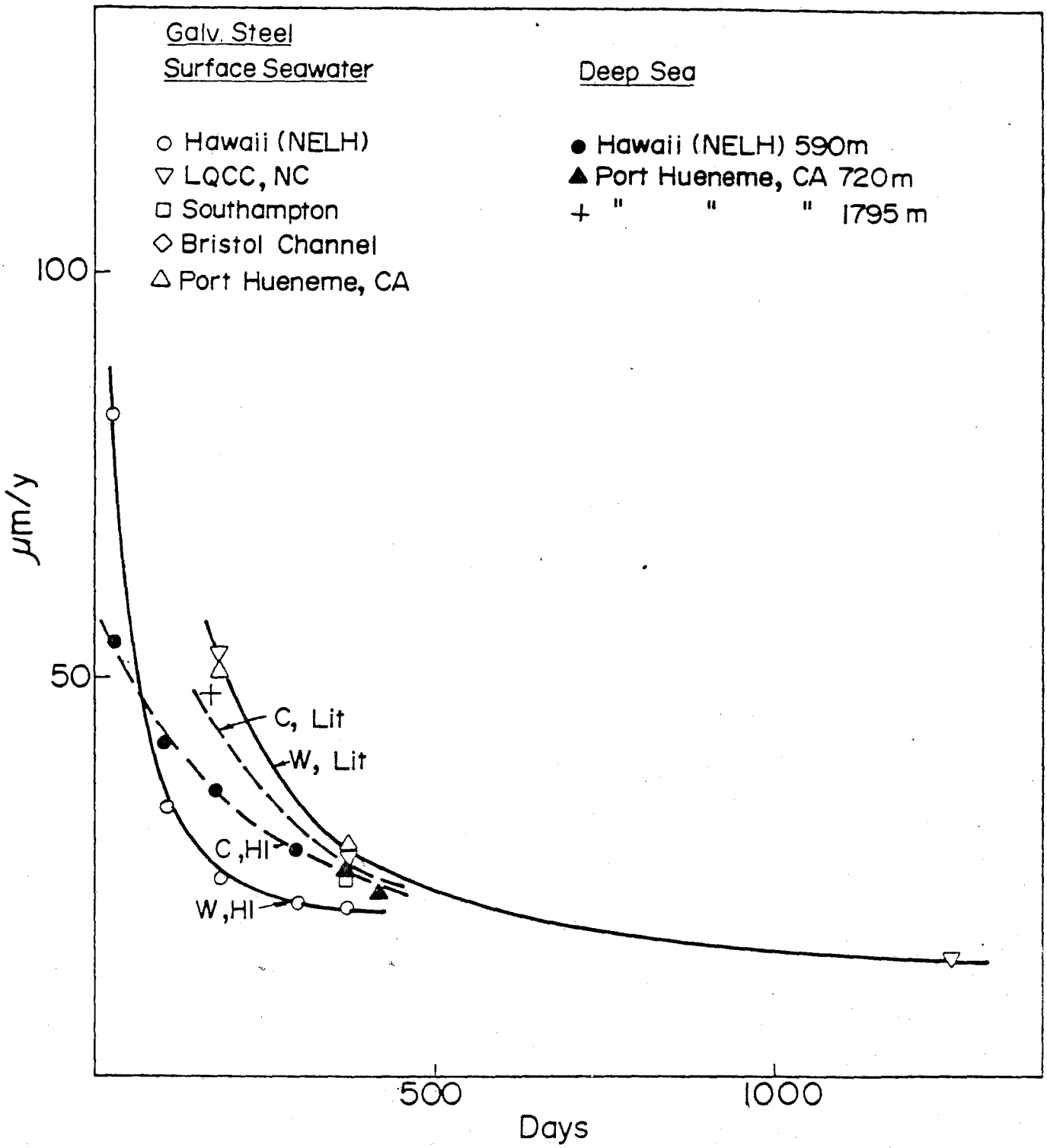

Fig. 7 Comparison of linear corrosion rate data from NELH with literature data.

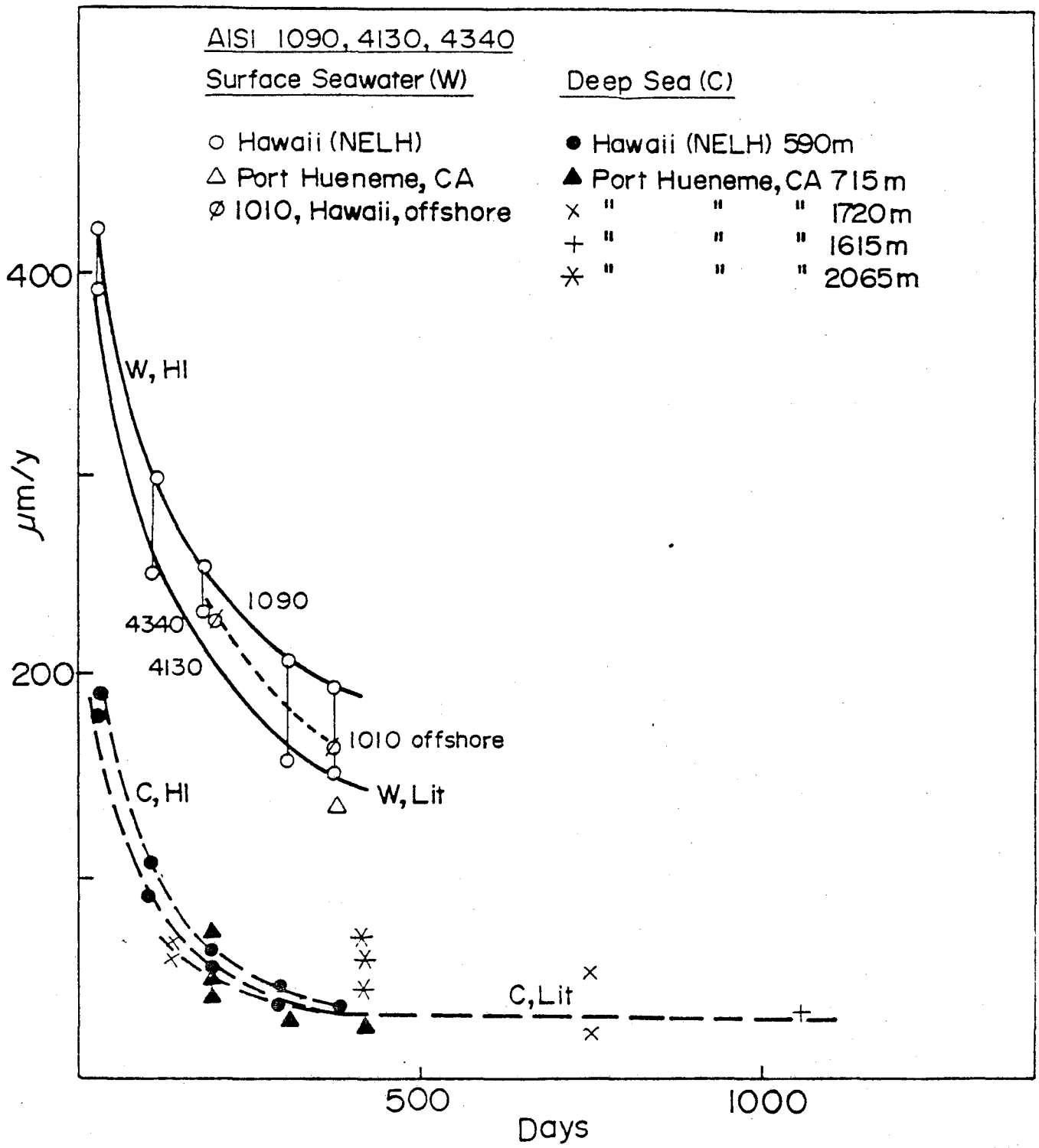

Fig. 8 Comparison of linear corrosion rate data from NELH for steels AISI 1090, 4130 and 4340 with data from Port Hueneme.

Lead: The cold water gives a slightly greater attack than the warm due to a greater rate during the early stage of exposure. In both waters a thin, tenacious, protective dark grey film forms early in the exposure period.

A comparison with literature data is shown in Fig. 9. The cold water data from Hawaii essentially coincide with the deep sea results from Port Hueneme, while the Hawaiian surface water rates are considerably lower than rates reported from other sites. It appears that a long-term rate of 2-4 μm/y is established in both Hawaiian waters after about 3 years. The same rate is obtained for the Port Hueneme deepsea exposures, while surface seawaters around the world establish a rate of 10-13 μm/y after 4 years. It has been suggested[8] that the low rate found in Hawaiian surface seawater is primarily due to its greater pH (lead corrosion is accelerated at lower pH-values) and possibly also due to the low water flow rates used in the tests.

In summary, long-term corrosion rates in Hawaiian surface waters are expected to be

- 15-20 μm/y for the coating on galvanized steel,
- 50-75 μm/y for the high-carbon steel, with a possibility of a higher rate, at 100-130 μm/y,
- 2-4 μm/y for lead.

In the deep ocean, the expected long-term rates are

- 20 μm/y for the coating on galvanized steel,
- 20-40 μm/y for high carbon steel, and
- 2-4 μm/y for lead.

These rates become established during the first 1-4 years of exposure.

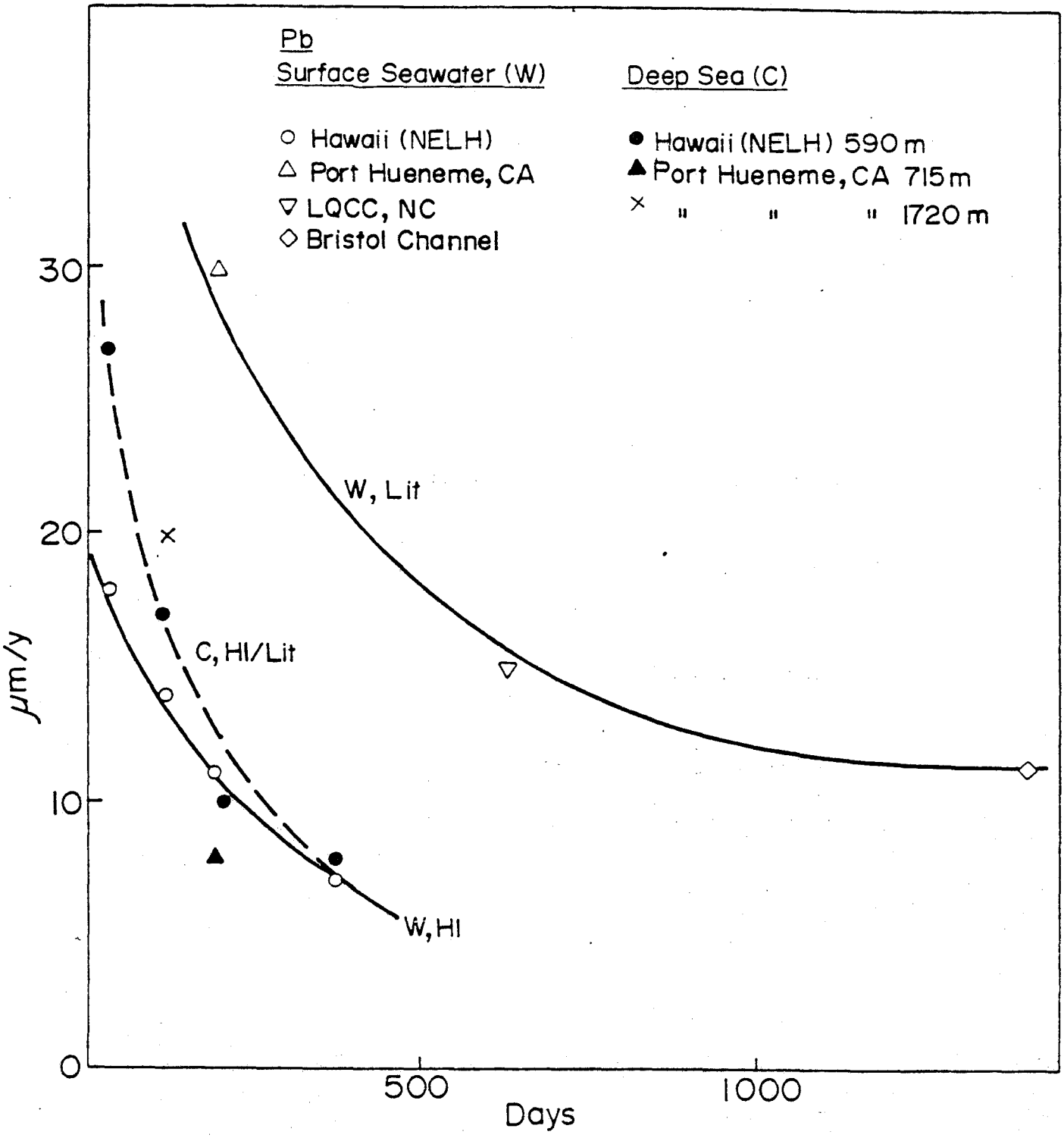

Fig. 9 Comparison of linear corrosion rate data from NELH for lead with literature data.

IV b. Tests With Cable Specimens

Some medium-term exposure tests with sections of a Pirelli cable were begun in 1985. The cable was a three-conductor cable. The inner parts of this cable were unaffected by the exposure tests and will be described only very briefly.

The copper conductors were shielded by EPR (ethylene propylene rubber) semi conducting compound, insulated by EPR insulation, and the insulation was again shielded by EPR semi conducting compound and screened by copper tape.

Three cores of the above make-up were separated by polypropylene fillers and bound with rubberized fabric tape to a diameter of 84.9 mm.

The outer layers, which are of more interest in the present context followed on top of the fabric tape:

- a bedding of 2 mm thick polypropylene yarn,
- a layer of bitumen
- a layer of 6 mm diameter galvanized armor wires of cold drawn AlSl 1025, zinc coat approximately 50 μm thick, and
- a serving of 3 mm thick polypropylene yarn, identical to the material which will be used in the HDWC cable.

The outer diameter of the cable was 106.9 mm and its weight 20.4 kg/m.

Three 0.45 m long sections were used for the exposure tests. The cut ends were covered with epoxy and duct tape. One sample was tested in the warm water trough, one in the cold water through, and one was mounted on the pipeline offshore at NELH. The latter was about 100 m from the cliff, 12 m below the surface, and 1.5 m above the bottom. The ASTM tests, mentioned earlier, were conducted at the same location. Each sample will be discussed separately below.

Sample from Warm Water Trough: this sample was exposed in slowly flowing surface seawater at 25-28°C, with a pH of 8.25 and fully saturated with oxygen. Exposure period was October 31, 1985 to June 28, 1987, or 605 days.

Upon removal the sample was dissected. Only the armor wires showed effect of the exposure, in the form of minor corrosion. The average loss of zinc coating was determined by chemical dissolution and weight changes. It was 5 μm for an average rate of 3 μm/y. This rate is much lower than the 15-20 μm/y measured on coupons in the troughs. The difference is clearly due to the protection offered by the polypropylene serving and the bitumen layer. It is expected that almost all the loss took place on the outer 50% of the wire diameter (i.e., the area not covered with bitumen). This would give an average corrosion rate of about 6 μm/y which still is low.

Sample from Cold Water Trough: This sample was exposed in slowly flowing water pumped from about 600 m depth. The temperature was 7-10°C, pH 7.6 and the oxygen content a low 1.1 ppm. Period of exposure was October 31, 1985 through October 30, 1987, or 2 years. Upon dissection it resembled the warm water sample, discussed above, with an average zinc coating loss of 6 μm, or at a rate of 3 μm/y. Assuming attack on only one-half the surface the rate becomes 6 μm/y, which again is considerably below rates for freely exposed galvanized steel.

Off-Shore Sample: this sample was exposed for 747 days, from Nov. 23, 1985 through Dec. 10, 1987. In this case the total coating loss was 18 μm, giving a distributed average rate of 8.8 μm/y and a half-area rate of 17.6 μm/y. This rate is similar to values expected for freely exposed galvanized steel. It is considerably greater than measured in the warm water trough, probably due to the strong ocean currents at the site.

IV c. Samples of Armor Wire

A number of corrosion tests were performed with pieces of the actual armor wire selected for the final HDWC design. The material is a cold drawn AISI 1085 steel of rectangular cross section, 10 mm x 3 mm. It is galvanized to a coating thickness of 75 μm and has a Vickers hardness of 525 k_s/mm^2.

The points of interest in this study were a) the corrosion rate of this material in seawater, especially in the early stages of exposure; b) the "throwing power" of the coating, i.e., its ability to protect a break in the coating; and c) the tendency for stress corrosion cracking. Samples were exposed both in the troughs at NELH and in the Materials Engineering Laboratories at the University of Hawaii. In the latter tests stagnant surface seawater was used at room temperature in a test vessel. The water was obtained from the Waikiki Aquarium.

Tests in the Laboratory: Twenty samples of armor wire, 34 mm long, were stripped of coating by immersion in HCl and subsequently exposed in stagnant seawater at room temperature. Weight loss was determined for exposure period of 0.5 to 24 h. The calculated average thickness loss is plotted in Fig. 10. The 24 h value corresponds to an annual rate of 175 μm/y, which, in view of other data, seems reasonable for the early stage of attack. The one-hour corrosion is about 0.07 μm, which corresponds to an annual rate of 613 μm/y. The actual one-hour corrosion determined here is substantially lower than the value obtained from back extrapolation of equation (6) which was derived from longer-term tests of AISI 1090. That value is 0.40 μm (vs. 0.07 μm). The difference is probably primarily due to uncertainties in the extrapolation from 1-10 month data to a 1 hour exposure time and only secondarily due to the small differences in exposure conditions.

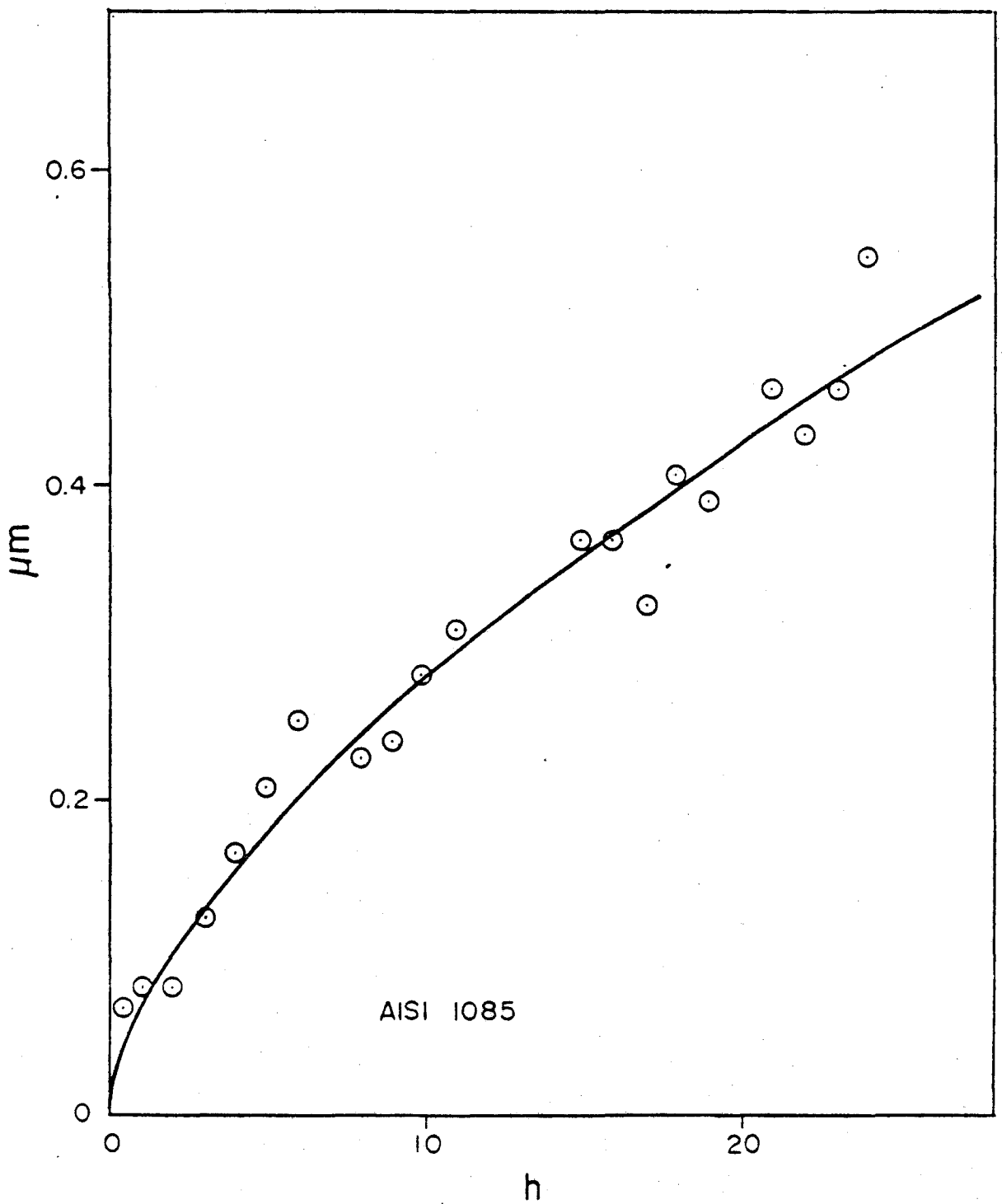

Fig. 10 Corrosion loss for armor wire exposed in stagnant seawater for short periods of time.

Tests in Warm Water at NELH: Armor wire samples were tested for their possible susceptibility to stress corrosion cracking in seawater. Both 2-point bending and U-bend samples were used with various degrees of coating removal. Details of samples and results are given in Table 3. The samples were exposed in the troughs at NELH for 202 days from 4/10/87. After removal the tension side was cleaned and examined by low power microscopy. No cracks were found.

TABLE 3
202-Day Stress Corrosion Test Samples

Type	Length mm	Max. stress psi	Zn* Removed	Coating Loss Rate, μm/y +	
				Cold Water	Warm Water
2-Point Bending (ASTM G39-70)	254	50,000	0	41.5	36
			51 mm**	110	116.5
			full length**	121	115.5
U-bend (ASTM G30-79) R = 8.5 mm	93	125,000	0	58	22.5
			51 mm**	69.5	27
			full length**	106	33
			100%	1.3++	8.5++

* Zn removal by H Cl + 56 Cl_3 according to ASTM G90-69
** On tension side only
\+ Weight loss converted to coating loss. In reality there is some corrosion of the bare steel also.
++ Steel corrosion

Samples for general corrosion were also tested. These had various degrees of coating removal, over 30, 60 or 100% of the specimen length. They were exposed in the troughs for 67 and 189 days from 4/23/87. The results are summarized in Table 4.

TABLE 4

Tests for General Corrosion

	μm/y in Cold Water		μm/y in Warm Water	
Exposure Period	67 days	189 days	67 days	189 days
Zn corrosion				
0% removed	67.5	32	36.5	7
30% removed	113	58	25	0.5
60% removed	810	462	59	24.3
Steel Corrosion (100% Zn removed)	60	44	101.5	100

The data for both the fully galvanized and the completely bare steel in the cold water are consistent with the coupon test data discussed above, while the warm water results are somewhat lower. For the samples which have part of the coating removed, the corrosion rate of the coating is greatly accelerated in the cold water. When even a small part of the coating is removed before immersion, the remaining zinc does not fully protect the steel. This is particularly pronounced in the cold water because of reduced throwing power. When the total weight loss is calculated as thickness loss for the coating only, extremely high values result.

IV d. Summary of Corrosion Data

The corrosion tests have shown the following:

- no cracking is expected due to stress corrosion or hydrogen embrittlement at cathodic sites,
- the intact zinc coating, if freely exposed, will corrode at a long-term rate of 15-20 μm/y in the surface seawater and 20 μm/y in the deep sea,
- bare armor wire corrodes at long-term rates of about 75 μm/y in the warm water and 30 μm/y in the cold,

- when the polypropylene yarn serving and the bitumen layer on the bedding are intact the corrosion rate of the zinc is reduced by a factor of about three,

- if the zinc coating is removed in local areas the corrosion rate increases drastically. The throwing power is less in cold water than in warm and the galvanic effect increases rapidly as the damage zone exceeds 40-50 mm in length. Even coating damage on one side only results in significant increase in galvanic corrosion and consequent rapid consumption of the zinc coating, and

- short-term corrosion rates of the bare steel in warm seawater are around 615 μm/y during the first hour and 175 μm/y during the first day.

V. ABRASION TESTS

Several different types of abrasion tests were utilized, ranging from sliding against dry abrasive papers to repeated sliding against pillow lava rocks immersed in seawater.

V. a Abrasion by SiC Abrasive Paper

In order to determine the possible effects of wire orientation on abrasive wear rates scoping tests were carried out using 120 grit silicon carbide abrasive paper, which has a mean grit size of 120 micrometers. Since the armor wire has rectangular cross section and is heavily cold drawn the mechanical properties may vary with direction. There are six possible orientations of interest, as shown in Figure 11. The ASTM notation system for fracture mechanics has been adapted for use here. The arrows indicate direction of sliding, i.e., direction of the abrasion grooves.

The tests were all conducted dry at a sliding velocity of 3.0 cm/s on a track length of 1.42 m. Some tests were conducted with repeated sliding in the same track, while others utilized fresh paper for each pass. Specimen size was 34 x 10 x 3 mm and both galvanized and bare samples were tested. The wear was calculated as mm^3 of steel lost from weight loss measurements. The cutting force was averaged over each pass and the coefficient of friction was calculated.

Tests with Fresh Tracks: These tests were conducted with galvanized samples, except for one test with a bare sample (zinc removed). The results are plotted in Figure 12.

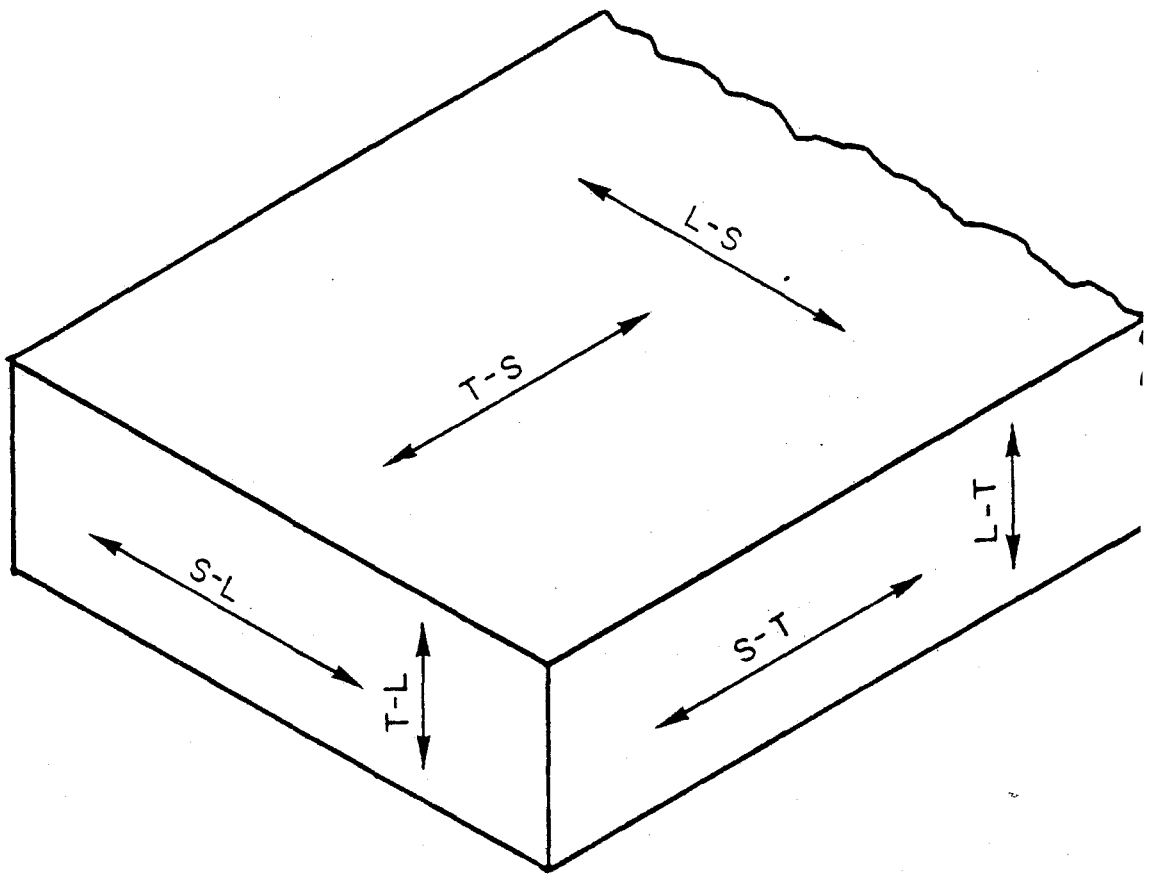

Fig. 11 Notations used to indicate sliding direction.

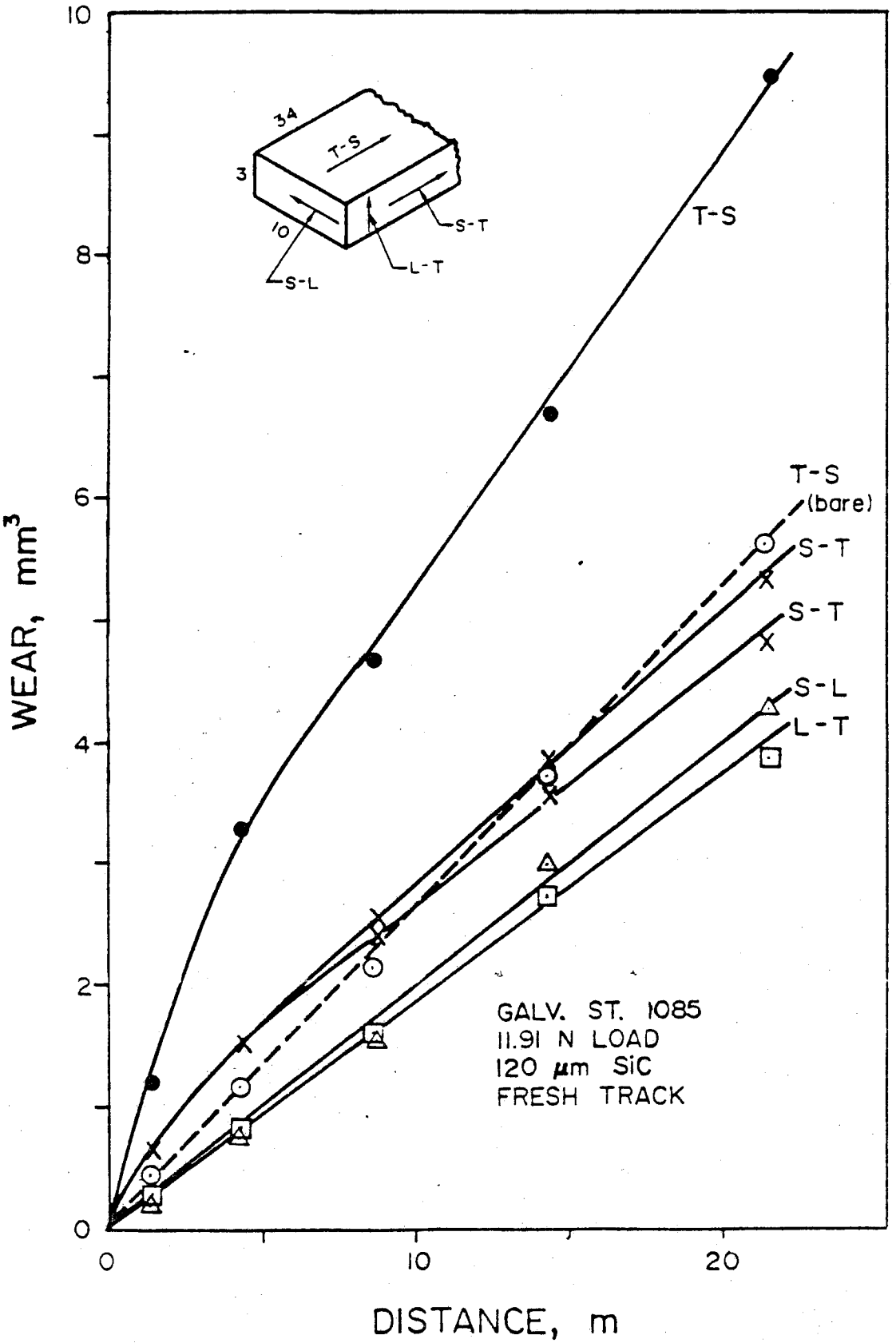

Fig. 12 Wear-distance curves for tests on fresh tracks of SiC paper for various sliding directions.

The coefficient of friction stayed essentially constant for each test and only the average values have been plotted. These range between 0.59 and 0.72, showing no clear correlation with specimen direction being abraded. An overall value of 0.66 appears to be reasonable, and is consistent with common literature values.

Since the tests were conducted with galvanized samples, some of the behavior seen is due to abrasion of the zinc in the early stages of testing. With 75 micrometers of zinc coating, the face corresponding to T-S has 25.5 mm^3 of zinc, S-T and L-T have 7.65 mm^3, while S-L has no zinc on the front face. Recalculated as mm^3 steel these numbers become 25.5, 7.65 and zero. With the long specimen size selected it is probable that complete contact was not achieved for the T-S and possibly the S-T directions, i.e., a combination of zinc and steel wear may be seen. Since the zinc is soft it will have little resistance to abrasive wear.

The curves for galvanized T-S and S-T show initial rapid wear, probably corresponding to zinc removal, followed by linear relations after 5m of sliding. The other directions show wear proportional to sliding distance, as is generally expected. Slopes of the lines are:

T-S	0.36 mm^3/m
T-S, bare	0.27
S-T (1)	0.23
S-T (2)	0.21
S-L	0.20
L-T	0.19

Of these, the T-S value is discarded because of the contribution of the zinc, as discussed above. The geometry and dimensions of the test specimens do not permit a direct, rigorous comparison of the data. If the wear rates are plotted vs. specimen length in the direction of sliding, see Figure 13, a slightly increasing trend is seen. This is not unexpected from the mechanics

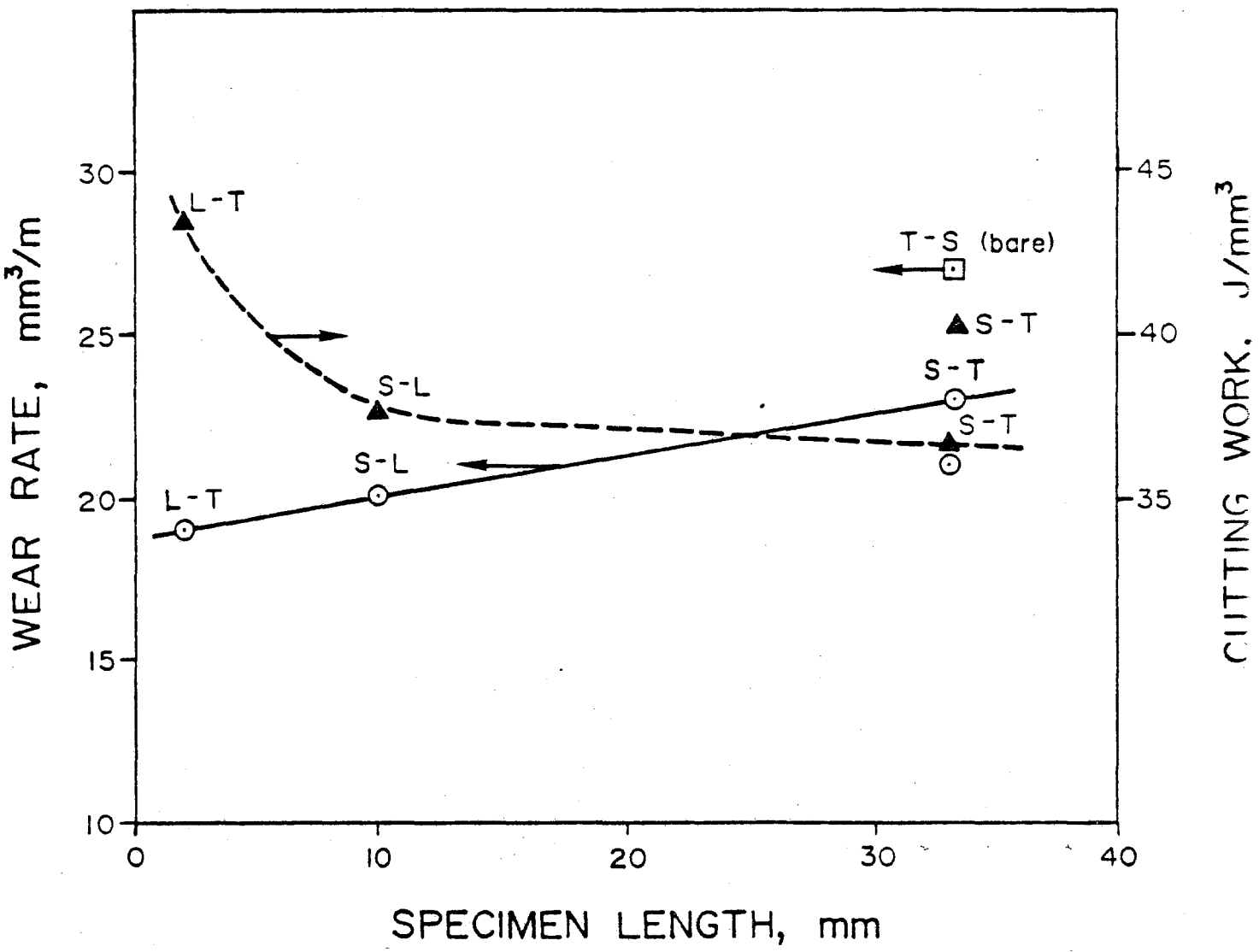

Fig. 13 Wear rate and cutting work vs. specimen length in direction of sliding, for abrasion by SiC paper.

of abrasion alone and indicates that there are no significant differences in abrasion properties between these three directions. The wear rate for the T-S direction is somewhat greater. This can be attributed to the greater width and lower contact pressure for this configuration. Again, the data do not indicate any significant variation in abrasion resistance with specimen orientation. This is seen more clearly in Figure 14, where wear rates have been plotted against contact area. The value for the very short dimension, L-T, lies below the general correlation here. Values for the galvanized samples have been adjusted to account for the 6% of the wear rate which is due to removal of zinc around the perimeter of the contact area.

The work expended in removing unit volume can be calculated from

$$CW = \frac{P \bullet \mu}{\dot{\omega}} \tag{8}$$

Where CW is the curring work (J/mm^3), P is the applied load (N), μ is the coefficient of friction and $\dot{\omega}$ is the wear rate (mm^3/m). The calculated values are

S-T (1)	36.41	N/mm^3
S-T (2)	40.26	
L-T	43.48	
S-L	37.63	

These values are also plotted in Figure 13. The cutting work drops rapidly as sample length increases to about 10 mm and then essentially levels off.

These experiments have shown that there are no significant differences in abrasion resistance between the various orientations of the armor wire and that a coefficient of friction of 0.66 and a max. wear of around 0.275 mm^3/m can be expected for abrasion by SiC abrasive papers.

Repeated Tests in Same Track: A number of tests were conducted in the same equipment but using the same track for each test. Samples were weighed

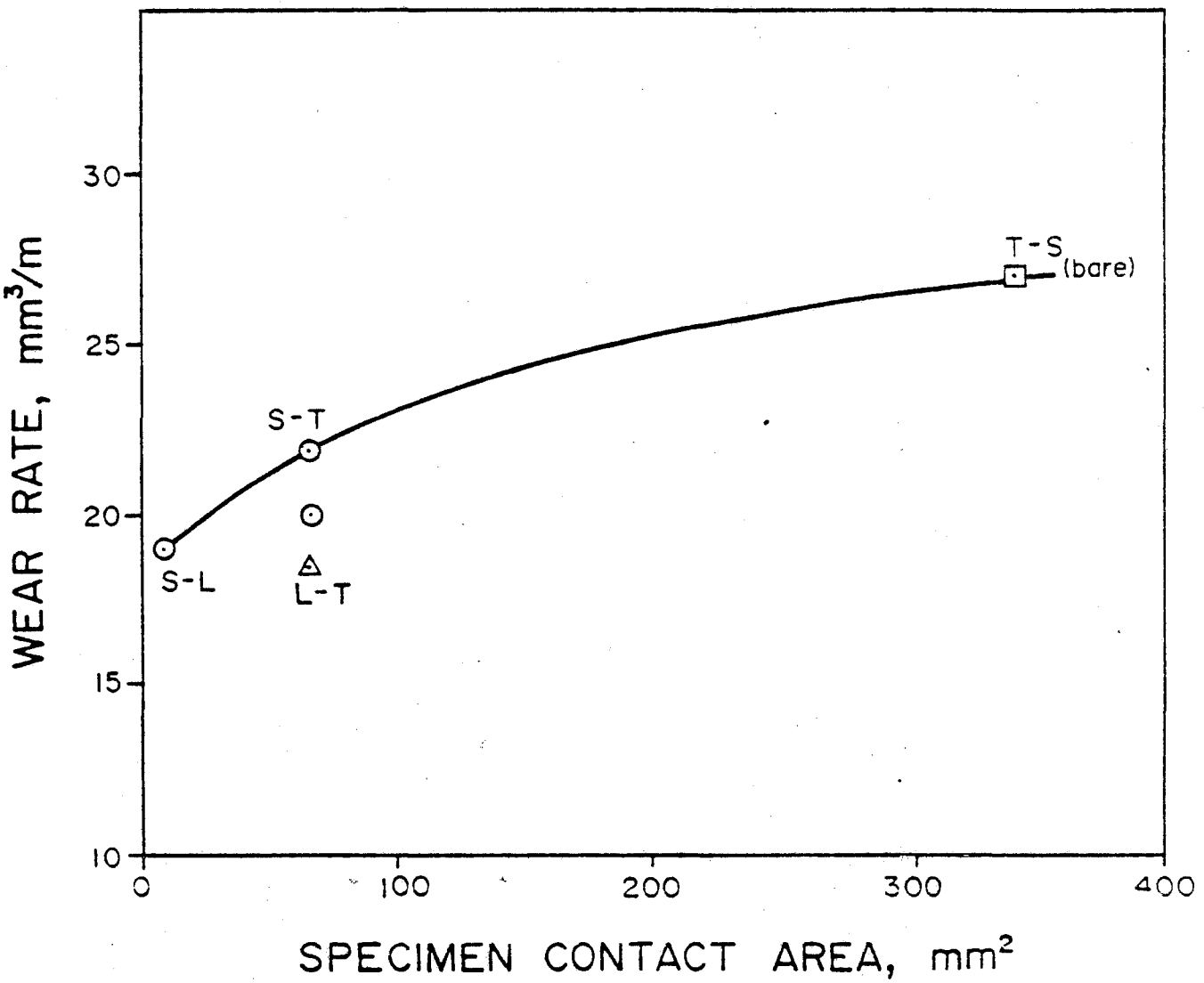

Fig. 14 Wear rate vs. contact area for abrasion by SiC paper.

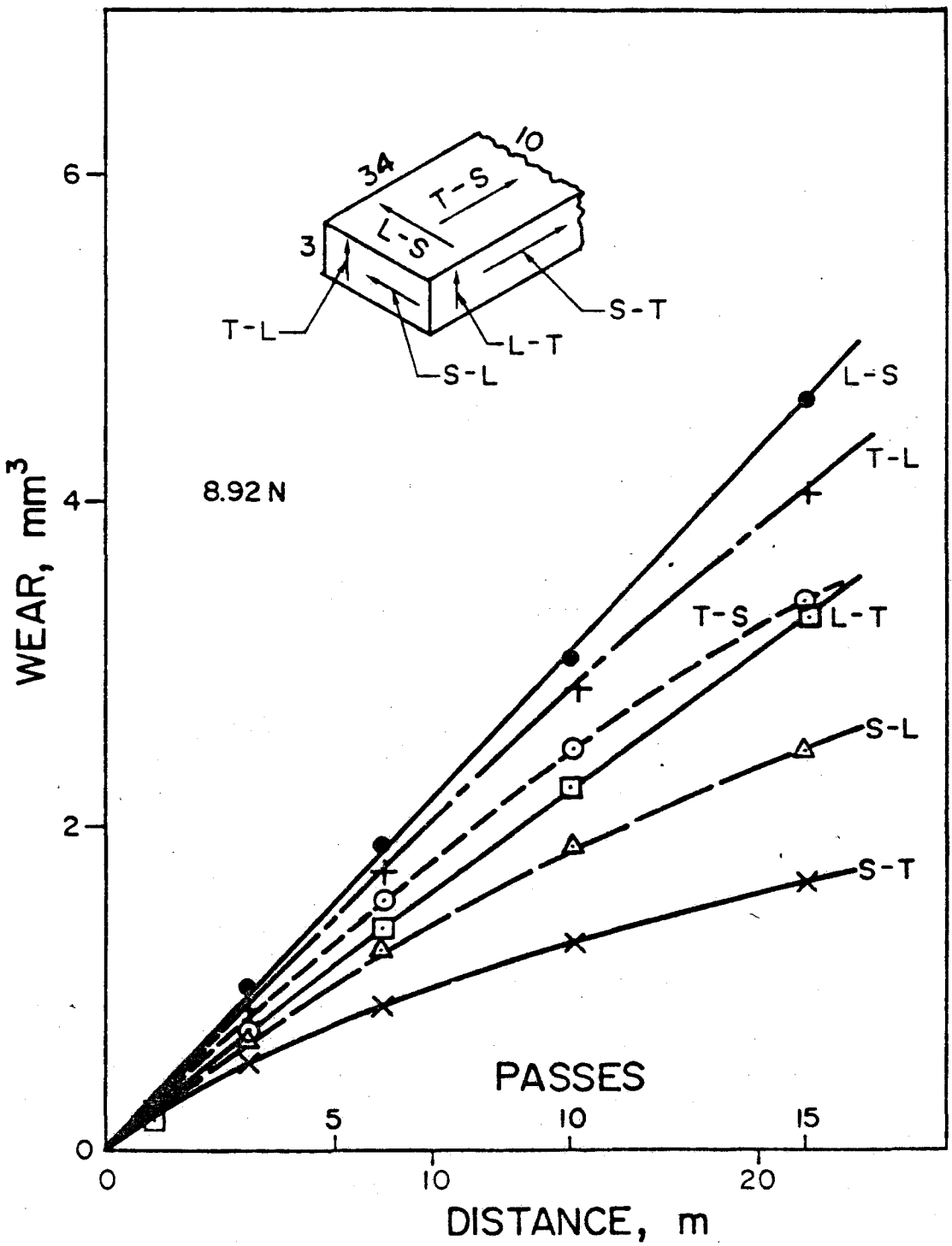

Fig. 15 Wear vs. distance of sliding in same track on SiC paper for different sample orientations.

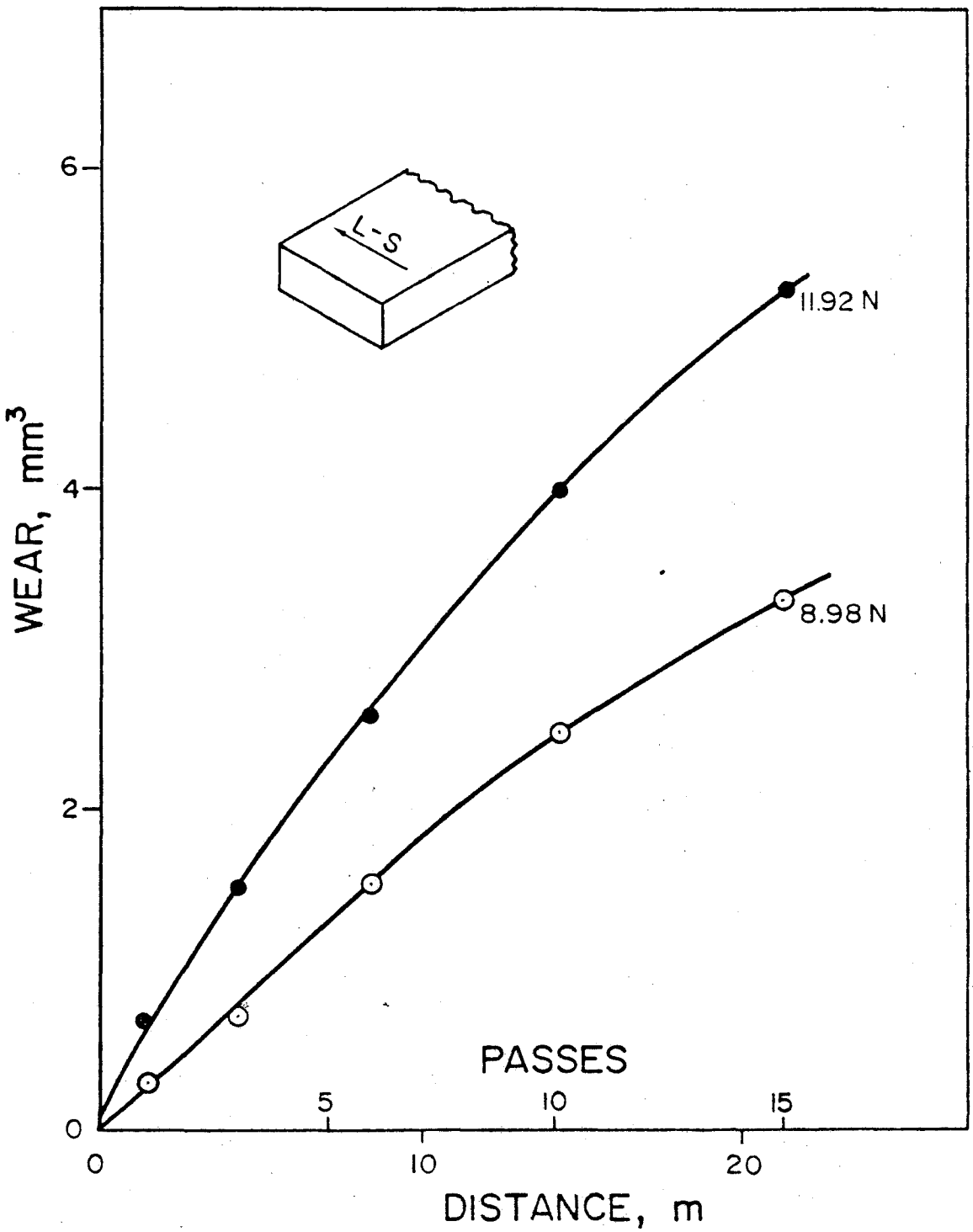

Fig. 16 Wear vs. distance of sliding in same track on SiC paper for two different loads.

after 1,3,6,10 and 15 passes in one direction over the 1.42 m long track. All samples had the zinc coating removed before test.

The wear data are plotted in Figs. 15 and 16. The results show a rather complicated interdependence of contact pressure, distance, and specimen length in the direction of sliding. Much of this behavior is due to wear of the abrasives. The data show no indication that the wire material's resistance to abrasion is in any way dependent on orientation.

V b. Abrasion of Basalt Rocks

Tests were conducted against two different types of rock:

- a deepsea channel rock from dredge #6 (see Fig. 3). This is a fine grained rock with only fine-scale porosity. Its density is 2.35 and its hardness is about 300 kg/mm^2 on the Vickers scale, and
- a rock collected from the shore at NELH. This rock has a significant amount of pores of 1-2 mm diameter. Its density is 1.96 and its Vickers hardness is about 600. It contains olivine grains of 0.2-0.4 mm diameter.

These two types of rock are thought to represent the various types expected in the Alenuihaha Channel. Since the hardness of the armor wire is 525 Vickers one might expect the shore rock to be much more abrasive than the channel rock. This was not the case, as shown below, probably because the low hardness of the channel rock may be due to its very fine porosity, which has little effect on abrasiveness.

The tests were conducted in seawater at room temperature. This was chosen because some rocks may microfracture more readily in the presence of moisture and because it would closely resemble actual conditions.

Two samples were tested together, and a common coefficient of friction was measured. Wear was determined by weight-loss measurements at intervals of

testing. The samples were slid back and forth in the same track of about 0.12 m length at a frequency of about 1200 round trip cycles/h.

Samples were tested in the galvanized condition, with the coatings removed on that 50% of the specimen which faced the rock, and bare, with all the coating removed. Removal was by chemical dissolution (HO + Sb_8Cl_3), followed by slight abrasion by 500 μm SiC paper. The 34 mm long samples of armor wire were tested in various directions relative to the direction of rolling.

In order to have a smooth run it was necessary to wear against a cut rock surface. In order to introduce a realistic surface roughness these cut surfaces were sandblasted before tests. This treatment had little effect on long-term results but was retained for all tests for purposes of reproducibility.

The data show some interesting trends when plotted in terms of wear as thickness of material removed as a function of contact pressure, for various values of specimen length in the direction of sliding. See Fig. 17 for low pressure levels and Fig. 18 for the high pressure range. Fig. 19 illustrates the effect of sliding distance at high pressure on the wear. The results show the following:

- shore rock is about 25% more abrasive than channel rock,
- wear increases almost linearly with distance, after an initial running-in period,
- wear increases with contact pressure, somewhat less than linearly,
- wear decreases as the specimen length is increased for the same contact pressure,
- typical wear loss at 2.7 MPa contact pressure for 3000 cycles or 720 m sliding are 220 and 140 μm vs. shore and channel rocks, respectively, and,
- coefficients of friction fall in the range 0.4 to 0.5, concentrated around 0.45.

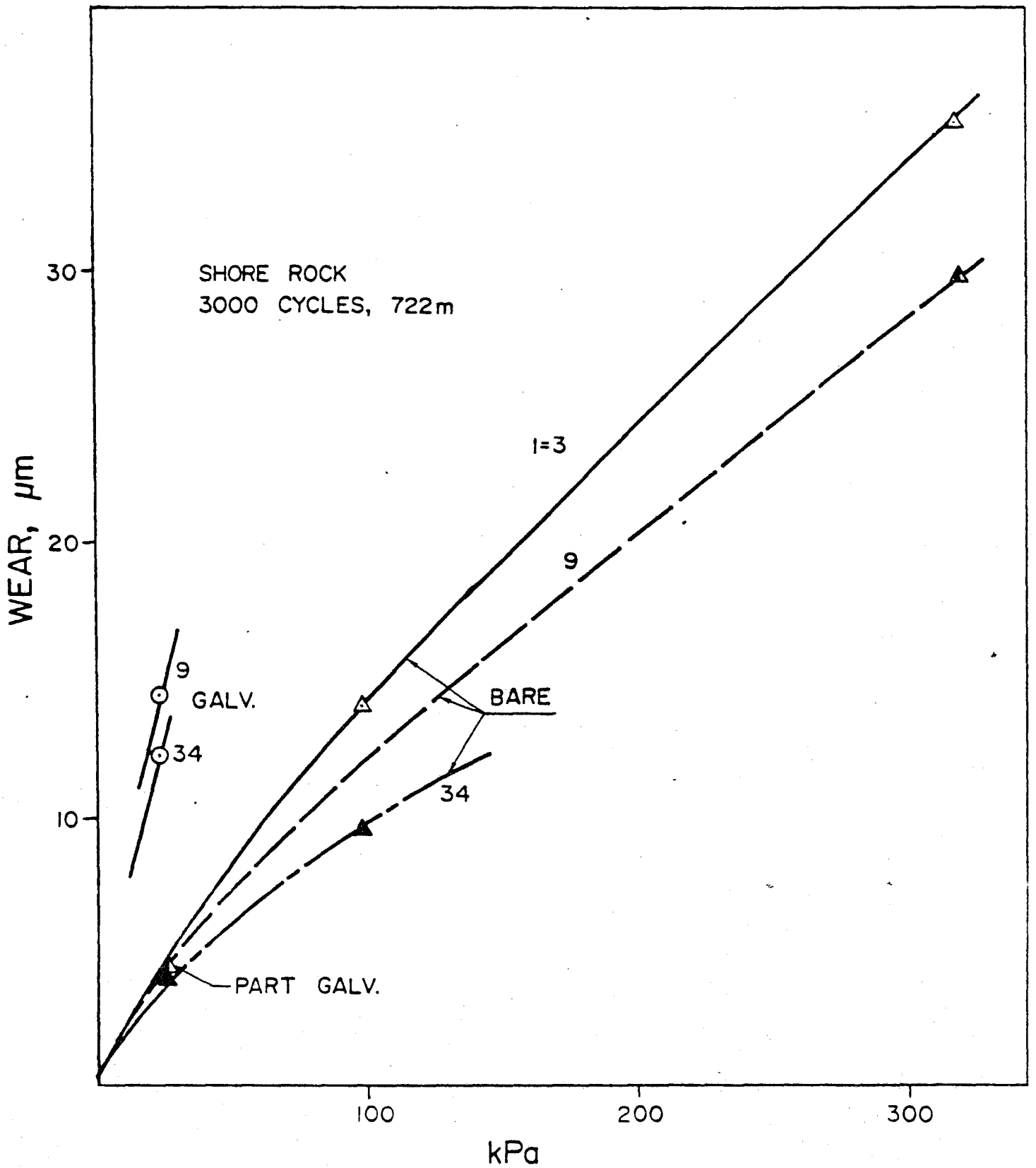

Fig. 17 Wear as thickness lost after 3,000 cycles or 722 m vs. contact pressure for different values of l, the specimen length in the direction of sliding.

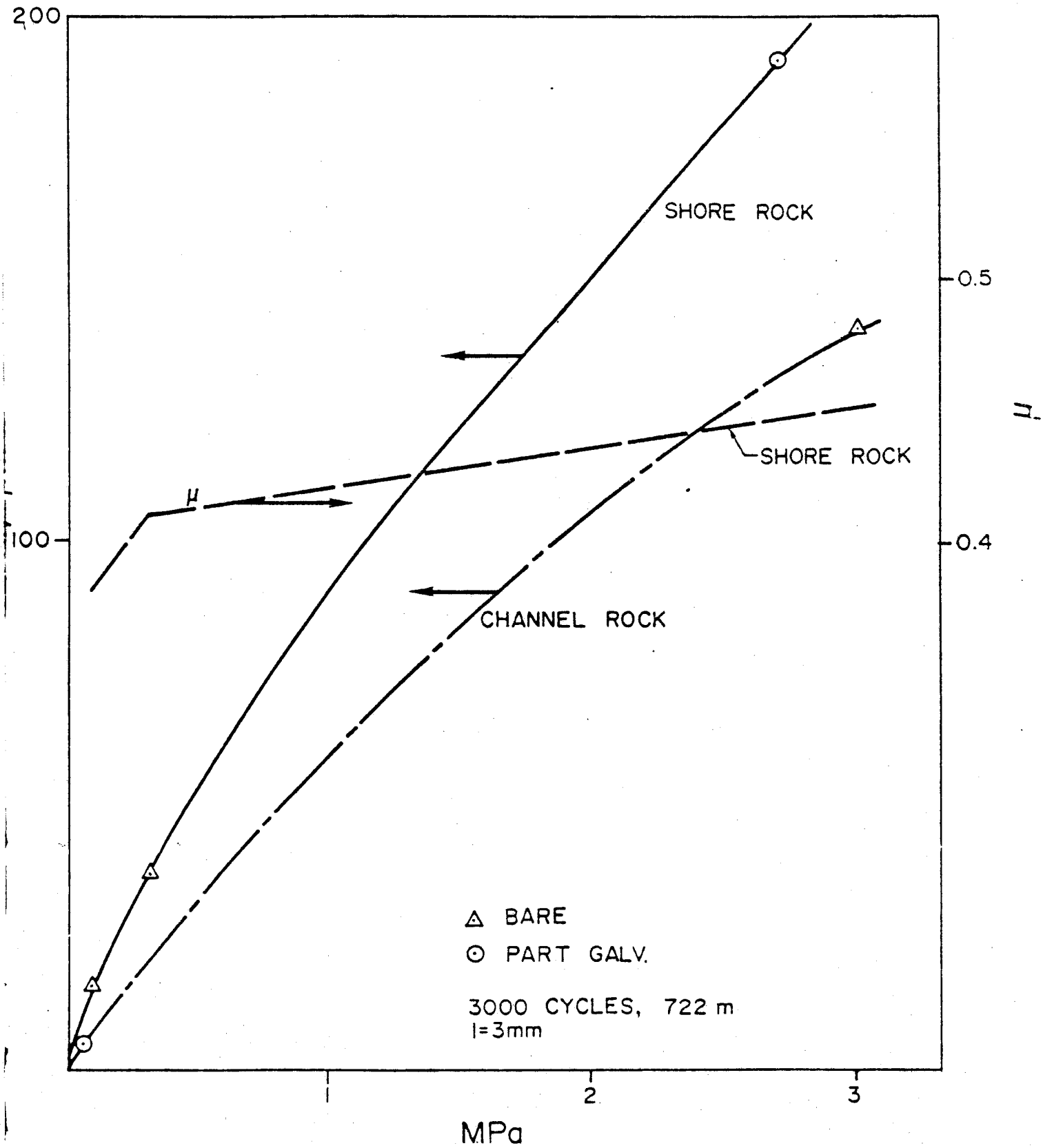

Fig. 18 Wear and coefficient of friction vs. contact pressure.

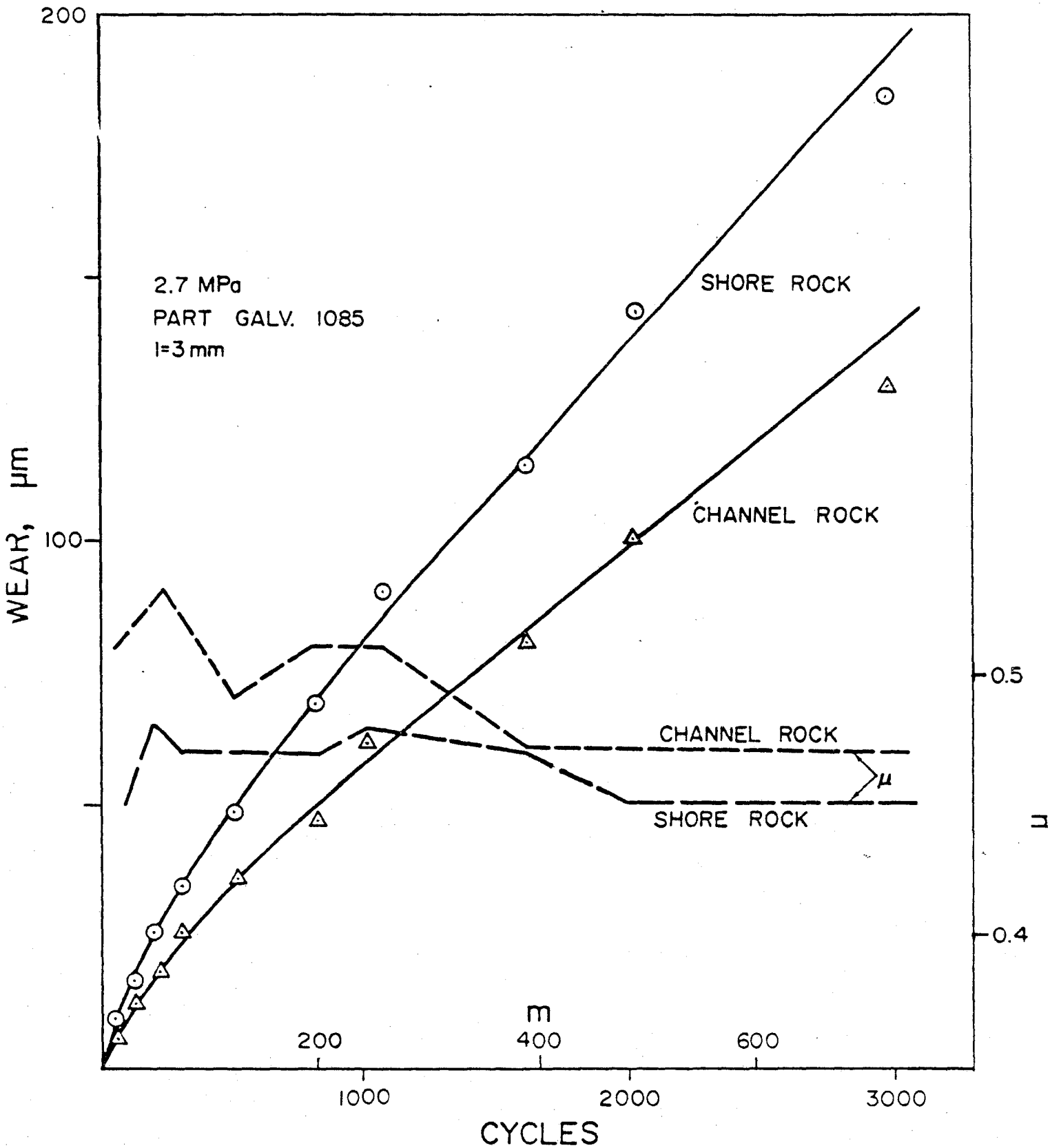

Fig. 19 Wear and coefficient of friction vs. sliding distance.

In order to obtain some information on the behavior of the armor wire-rock system under high contact stresses some tests were run with armor wires pressed against 90° angle edges of rock. These tests were run dry, with stroke lengths of 0.05 m. Weight loss of both rock and steel was determined.

The results are shown in Figs. 20 and 21. There is little difference in the rate of wear caused by the two different rocks. For extended testing the channel rock both causes more steel wear and itself wears more than the shore rock. The friction values, which were measured at intervals under a reduced load of 5N, declined from 0.4-0.45 to 0.25-0.3 during the course of the test. At the end of about 800 cycles or 25 m of sliding the rock had worn to a width of about 0.8 mm, such that the contact pressure was about 3.1-3.6 MPa, which is near the top of the range used in the seawater tests described above. At that point, the wear of the steel amounted to a depth of around 25-30 μm, and the wear rates were 0.45 μm/m against the channel rock and 0.2 μm/m against the shore rock. These values are in the general range found in the previous tests, where at 3MPa and 722 m sliding the wear rates were 0.2 and 0.25 μm/m against channel and shore rocks, respectively.

Tests with galvanized wires in the same configuration showed that the zinc coating was worn through quite rapidly, in 2-3 m of sliding, or 75-100 cycles.

V c. Abrasion by Crushed Basalt Slurry

It is conceivable that debris of crushed rock may remain in the wear scar and produce abrasion as a slurry. In order to assess the possible damage in this situation some slurry abrasion tests were carried out.

Shore lava rock was crushed and sieved to a particle size of 250-500 μm. 900 grams were mixed with 1 l of seawater to produce a slurry in which samples

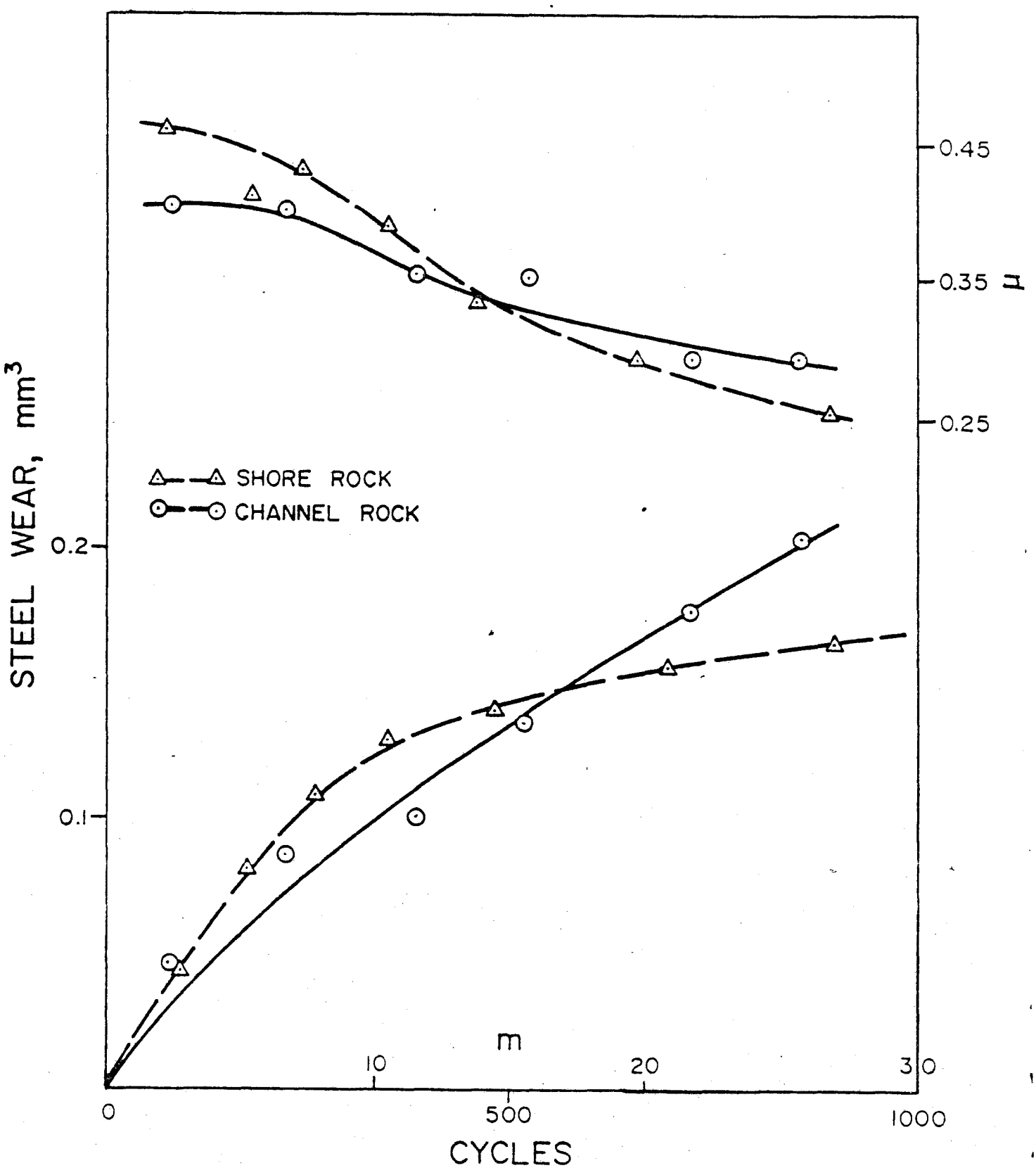

Fig. 20 Wear of bare armor wire abraded in the L-S direction against a 90° edge of rock under 46.4 N load.

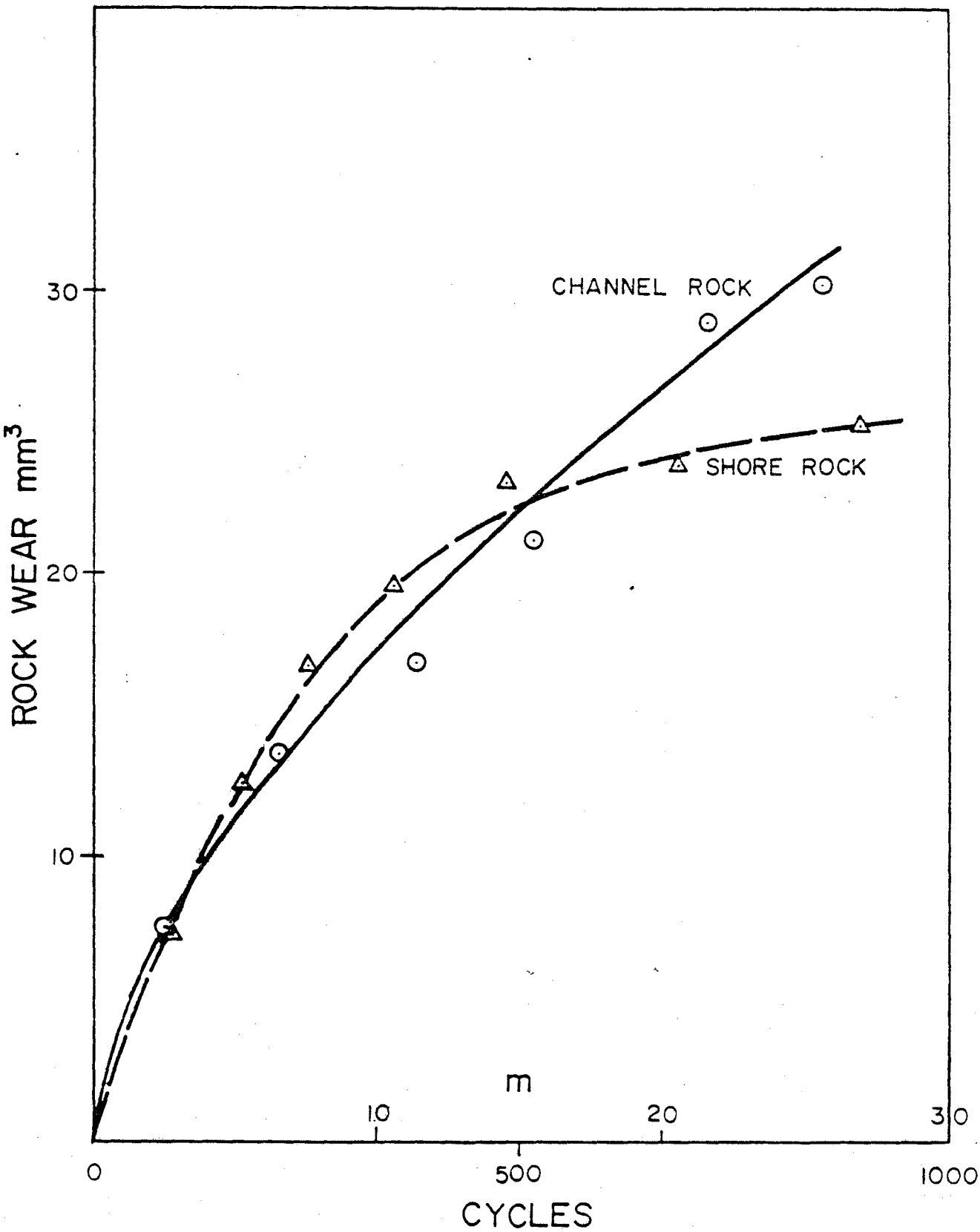

Fig. 21 Wear of rock under same conditions as in Fig. 20.

were abraded under a 9.5 N load. Details of the tester were given in our report for Phase II B. It is the same tester which was used in the seawater abrasion tests but with a different holder for the abrasives.

Results are shown in Fig. 22. Comparison with Fig. 17 shows that the slurry gives a wear rate which is about 3 times faster than abrasion by the solid rock face.

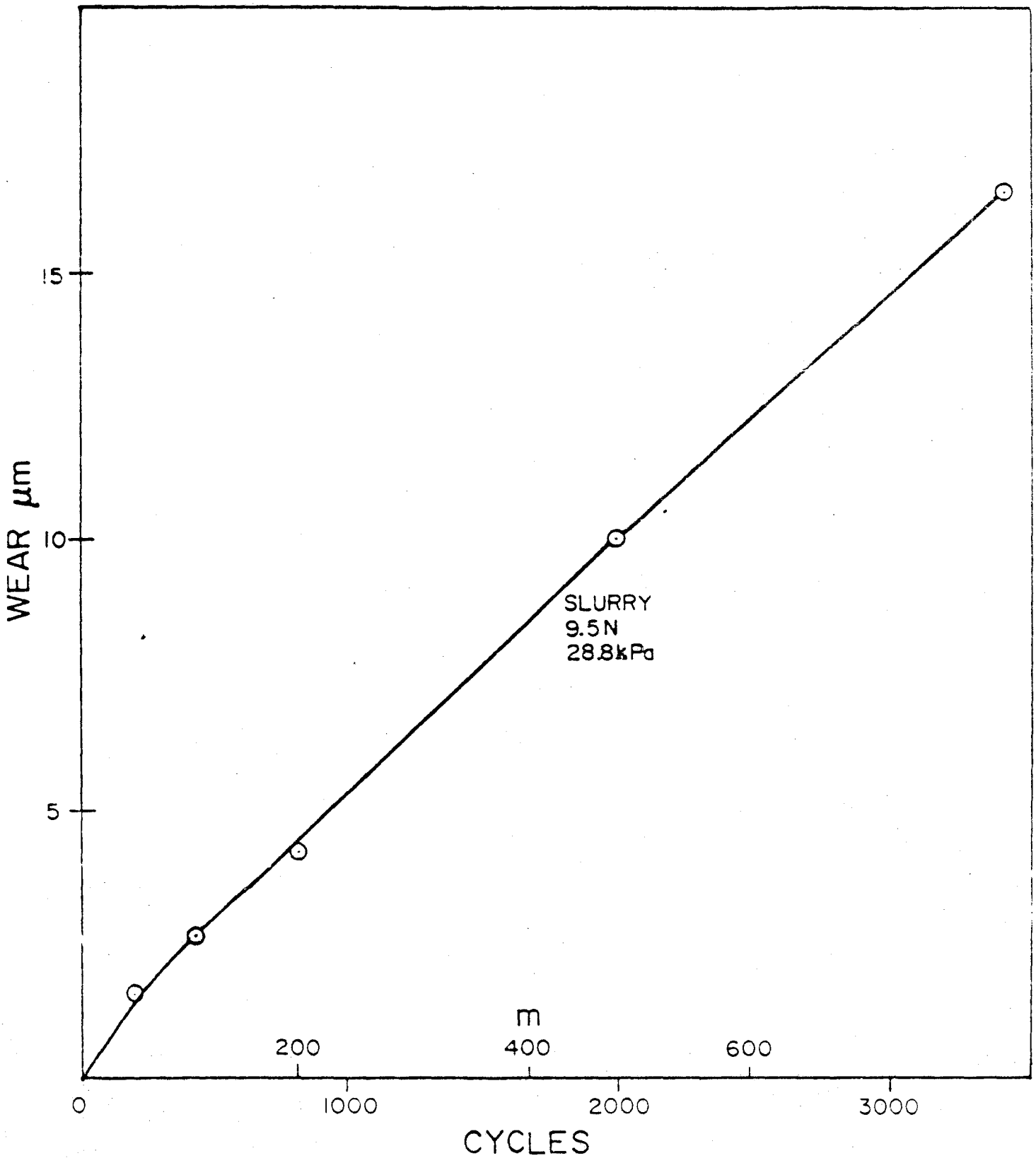

Fig. 22 Slurry abrasion of bare wire in the L-S direction at 28.8 kPa pressure.

VI. CORROSION-EROSION TESTS

If the corrosion film is allowed to build up with time it offers some protection against attack, and the corrosion rate decreases. If the film is constantly removed mechanically, there is a potential for rapid damage. The following tests were conducted in order to evaluate this possibility.

VI a. Erosion by Polyurethane Sheet

34 mm long samples of armor wire which had been completely or partially stripped of coating by chemical means as described above, followed by abrasion by 500 grit SiC paper, were used. They were exposed in stagnant seawater at room temperature in the laboratory, removed periodically and rubbed against a polyurethene sheet to dislodge the corrosion film. The results are shown in Table 5. It is seen that there is no effect of this mechanical damage on the rate of corrosion.

TABLE 5

Corrosion-Erosion by Polyurethene Sheet

Sample	Removal Interval, h	Total Exposure, h	Weight loss, ing
Bare	0.5 2 8	8 8 8	1.6 1.6 1.6
Part galv.	1/2 5	5 5	0.6 0.6

VI b. Erosion by Rock

The abrasion tester used for the seawater and slurry tests was modified to be controlled by a program which switched on the motor each 15 minutes, just long enough to go through one-half abrasion cycle (0.12 m). Tests were run in stagnant seawater for up to one week. The results are shown in Fig. 23. The rocks were sandblasted before the test. The partly galvanized sample had the zinc coating removed on the bottom (contacting) 50% of the 29 mm long sample.

The results show that the nature of the rock has little effect in this case. The greater wear shown by the part galvanized sample is probably due to the direct corrosion of the zinc in the seawater. For the bare wire the wear in a week is about 75 μm. Corrosion of the non-wearing surface is responsible for about 35 μm of that number (using a weekly rate of 1 μm), which leaves 45 μm due to abrasion and corrosion of the contacting surface. Results shown in Figs. 17 and 18 for the same number of cycles and the same contact pressure (but a much shorter period of testing) gave a loss of 3-5 μm. Thus, the corrosion of renewed fresh surface during the week has contributed most of the loss, in the order of 35-40 μm, or 0.1 μm/cycle.

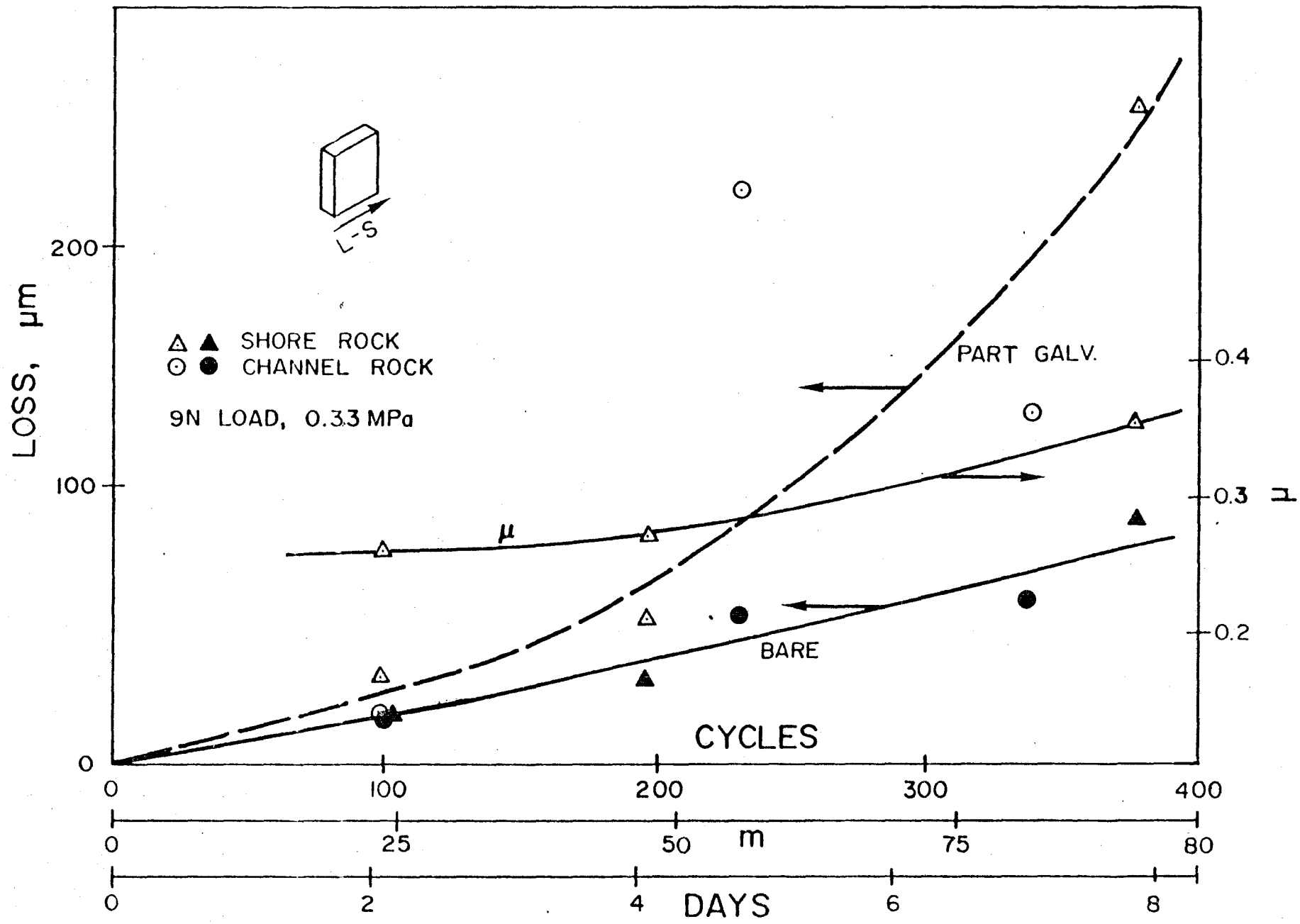

Fig. 23 Corrosion-erosion in stagnant seawater at room temperature.

VII. DAMAGE SCENARIOS

VII a. Straight Corrosion of Undamaged Cable

For an undamaged cable which has the serving and the bitumen intact the sequence of damage may be as follows:

- corrosion of the galvanized zinc coating at 6 $\mu m/y$ for about 15 years,
- corrosion of the steel armor wire at about 40-50 $\mu m/y$ from all sides for 30 years for complete loss of the first layer of wires. At the same time the second layer would experience some damage, but substantially less,
- even if water penetrates to the lead sheath, it has a straight corrosion life of well over a hundred years.

While the above corrosion rates are for cold water and undoubtedly will increase somewhat at the operating temperature of 60°C, there appears no reason to expect premature failure for this case.

VII b. Straight Corrosion of Damaged Cable

If the polypropylene serving is damaged during deployment the following scenario could be expected:

- corrosion of the front zinc coating at 20 $\mu m/y$ for 4 years,
- galvanic corrosion of the back zinc coating at possibly 75 $\mu m/y$ for 1 year,
- corrosion of the steel at 70-100 $\mu m/y$ for loss of the outer layer of armor wires after about 15 more years, for a total of about 20 years.

The inner layer of armor wire would still be well protected and would corrode at the slow rate discussed in section VII a. Thus, in this case too, there is no reason to expect premature failure.

VII c. Straight Abrasion

If the cable catenary is abraded by rock, the wear will soon remove the polypropylene serving and the zinc coating in the contact zone. The coefficient of friction between armor wire and basalt in seawater is 0.35-0.45. According to Fig. 6 this means a possible combination of excursion and load at the contact point which varies linearly from 0.47 m (see "note added in proof," p. 62) at 0 kg to 0 m at 540 kg.

$$h = 0.47 \left(1 - \frac{L}{540}\right) \qquad (9)$$

where h is the excursion in m and L is the contact load in kg.

Some worst-case estimates are shown in Table 6. For three different contact loads the excursion has been calculated from equation (9), the total travel in 30 years under this load is a max. of 87,600 x h. The wear at 3 MPa is obtained from Figs. 17 and 18 as about 200 μm in 722 m for a very short sample. Reducing to 150 μm for a longer sample and using the distances calculated yields values of up to 7 mm of wear.

The contact pressure of 3 MPa was chosen as a probable steady state max. value because the rock tested soon reached that contact stress. If, on the other hand, the rock remains reasonably sharp, with a contact of 5 mm width over 40 mm of the circumference, then much greater wear values are expected, as also outlined in Table 6.

TABLE 6*[1]
ESTIMATED WORST-CASE ABRASION

Contact load, kg	500	300	100
Excursion, m	0.035	0.21	0.38
Travel in 30 y, m	3,066	18,396	33,288
Wear at 3 MPa, μm	644	3,863	6,990
Pressure on 40 x 5 mm Contact area, MPa	25.5	14.7	5.1
Wear for same, μm	515	19,315	11,883
General corrosion 30 x 2 x 30, μm	1,800	1,800	1,800
Corrosion-erosion 4 x 365 x 30 x 0.05 μm	2,190	2,190	2,190

VII d. Combined Effects*

Generally speaking, the bottom rocks are quite smooth and rounded and significantly lower contact stresses than above will generally be expected. At 1.5 MPa for the 100 kg load the 30 year wear is 3,500 μm. To this should be added general corrosion of about 1,800 μm and corrosion-erosion of 0.05 μm per pass, or 2,200 μm. The total then is about 7,500 μm. The radial distance from the outer diameter of the armor wire to the outer diameter of the lead sheath is 14,600 μm.

It would therefore appear that the cable can survive, for its 30-year design life, the envisioned conditions of corrosion, abrasion, and corrosion-erosion.

1*see "note added in proof," p. 62)

Note Added in Proof

After completion of the study some results from recent measurements of bottom currents were made available.*[2] It was found that in 99.974% of the time the current is less than 0.51 m/s. This current produces a drag on the cable of 2 kg/m, instead of the 7 kg/m used in this study*.

With this new information the corrected drag on the span (p. 19) is (2-F/30) and equation (2) becomes

$$h = 0.1333 - F \cdot 0.0022 \qquad (21)$$

The limiting excursion in Fig. 6 then becomes 0.1333 m. Table 6 has been revised accordingly as Table 7, below.

TABLE 7

ESTIMATED WORST-CASE DAMAGE, REVISED

Contact load, kg	500	300	100	50	10
Excursion, m	0.01	0.06	0.108	0.121	0.131
Travel in 30 y, m	876	5,256	9,461	10,600	11,476
Wear at 3 MPa, μm	182	1,092	1,966	2,202	2,384
Pressure on 40 x 5 mm					
Contact area, MPa	25.5	14.7	5.1	2.55	0.51
Wear for same, μm	1,547	5,351	3,342	1,872	405
General corrosion, μm		1,800			
Corrosion-erosion, μm		2,190			

2*J. P. Walsh, in memo to K. T. Morikami, 3/8/88

The combined damage effects for the most of the worst-case scenarios is then 5,300 μm due to wear, 1,800 μm due to corrosion, and 2,200 μm due to corrosion-erosion, for a total damage of up to 9,300 μm. If damage proceeds as indicated by the line A-A in Fig. 2, i.e., if the cable does not twist as damage progresses, one would expect the wear scar to cut through the outer layer of armor wires and to cut well into the second layer. However, as the contact area will always contain a large amount of steel one would expect the distance worn from the outer diameter of the outer layer of armor wires to be a maximum of the 9.3 mm mentioned above. Since the radial distance to the lead sheath is 14.6 mm, it would appear that wear will not destroy the cable's electrical integrity. Whether this amount of damage will seriously affect the mechanical integrity of the cable should probably be considered separately.

VIII. ACKNOWLEDGMENTS

We are grateful to the staff at NELH, in particular Dr. Tom Daniel and Mr. Jan War for assistance in the on-shore and off-shore exposure tests; to Miss Tracy Kazunaga for performing many of the measurements; to Mrs. Kaye Fuller for typing the manuscript; and to our contract monitors, Mrs. Lois Nagahara at the Hawaii Natural Energy Institute and Mr. George Krasnick at Parsons Hawaii.

IX. REFERENCES

1. Hawaii Deep Water Cable Program, Phase II, Executive Summary, April 1982.

2. Pirelli Cable Corp. and Societa Cavi Pirelli, "Hawaii Deep Water Cable Program, Phase II, Cable Catenary Study," May 1986.

3. ASTM G75-82, "Test Method for Slurry Abrasivity by Miller Numbers."

4. G.A. MacDonald and A. T. Abbott, Volcanoes in the Sea, University of Hawaii Press, 1970.

5. Handbook of Chemistry and Physics, 57th ed., 1976-77, pp. C791-800.

6. J. Frisbee Campbell, "Hawaii Deep-Water Cable Program. Phase II: At-Sea Route Surveys," Hawaii Institute of Geophysics, August 19832.

7. J. Larsen-Basse and A. Tadjvar, "Behavior of Some Polymers Subjected to Slurry Abrasion Under Simulated Submarine Conditions," Wear of Materials 1987, v. 2, K. C. Ludema (ed.), ASME 1987, 709-715.

8. J. Larsen-Basse and Young-Ho Park, "Corrosion in Slowly Flowing OTEC Seawater: A One-Year Study," CORROSION '88, Paper # 395, NACE 1988.